are associated with increased DNA synthesis and reduced $p27^{Kip1}$ expression in the vasculature of hypertensive rats. Circ Res, 2001; 89: 488-495
23) Laufs U, Adam O, Strehlow K, Wassmann S, Konkol C, Laufs K, Schmidt W, Böhm M, Nickenig G: Down-regulation of Rac-1 GTPase by Estrogen. J Biol Chem, 2003; 278: 5956-5962
24) Iwai M, Chen R, Li Z, Shiuchi T, Suzuki J, Ide A, Tsuda M, Okumura M, Min LJ, Mogi M, Horiuchi M: Deletion of angiotensin II type 2 receptor exaggerated atherosclerosis in apolipoprotein E-null mice. Circulation, 2005; 112: 1636-143
25) Aikawa M, Rabkin E, Sugiyama S, Voglic SJ, Fukumoto Y, Furukawa Y, Shiomi M, Schoen FJ, Libby P: An HMG-CoA reductase inhibitor, cerivastatin, suppresses growth of macrophages expressing matrix metalloproteinases and tissue factor in vivo and in vitro. Circulation. 2001; 103: 276-283
26) Sakamoto T, Ishibashi T, Sugimoto K, Sakamoto N, Ohkawara H, Niinuma M, Nagata K, Kamioka M, Sugimoto N, Watanabe A, Kurabayashi M, Takuwa Y, Maruyama Y: RhoA-dependent PAI-1 gene expression induced in endothelial cells by monocyte adhesion mediates geranylgeranyl transferase I and Ca^{2+} signaling. Atherosclerosis, 2007; 193: 44-54
27) Ishibashi T, Nagata K, Ohkawara H, Sakamoto T, Yokoyama K, Shindo J, Sugimoto K, Sakurada S, Takuwa Y, Teramoto T, Maruyama Y: Inhibition of Rho/Rho-kinase signaling downregulates plasminogen activator inhibitor-1 synthesis in cultured human monocytes. Biochim Biophys Acta, 2002; 1590: 123-130
28) Nagata K, Ishibashi T, Sakamoto T, Ohkawara H, Shindo J, Yokoyama K, Sugimoto K, Sakurada S, Takuwa Y, Nakamura S, Teramoto T, Maruyama Y: Rho/Rho-kinase is involved in the synthesis of tissue factor in human monocytes. Atherocslesrosis, 2002; 163: 39-47
29) Cordle A, Koenigsknecht-Talboo J, Wilkinson B, Limpert A, Landreth G: Mechanisms of statin-mediated inhibition of small G-protein function. J Biol Chem, 2005; 280: 34202-34209
30) Liao JK, Laufs U: Pleiotropic effects of statins. Annu Rev Pharmacol Toxicol, 2005; 45: 89-118
31) Yoshida M: Potential role of statins in inflammation and atherosclerosis. J Atheroscler Thromb, 2003; 10: 140-144
32) Yamada S, Ito T, Adachi J, Ueno Y, Shiomi M: Decreased arterial responses in WHHL rabbits, an animal model of spontaneous hypercholesterolemia and atherosclerosis. Exp Anim, 2002; 51: 493-499
33) Mollnau H, Schulz E, Daiber A, Baldus S, Oelze M, August M, Wendt M, Walter U, Geiger C, Agrawal R, Kleschyov AL, Meinertz T, Münzel T: Nebivolol prevents vascular NOS III uncoupling in experimental hyperlipidemia and inhibits NADPH oxidase activity in inflammatory cells. Arterioscler Thromb Vasc Biol, 2003; 23: 615-621

Human C-Reactive Protein Does Not Promote Atherosclerosis in Transgenic Rabbits

Tomonari Koike, PhD*; Shuji Kitajima, DVM, PhD*; Ying Yu, PhD; Kazutoshi Nishijima, DVM, PhD; Jifeng Zhang, MS; Yukio Ozaki, MD, PhD; Masatoshi Morimoto, DVM, PhD; Teruo Watanabe, MD, PhD; Sucharit Bhakdi, MD, PhD; Yujiro Asada, MD, PhD; Y. Eugene Chen, MD, PhD†; Jianglin Fan, MD, PhD†

Background—Although there is a statistically significant association between modestly raised baseline plasma C-reactive protein (CRP) values and future cardiovascular events, the debate is still unsettled in regard to whether CRP plays a causal role in the pathogenesis of atherosclerosis.

Methods and Results—We generated 2 lines of transgenic (Tg) rabbits expressing human CRP (hCRP). The plasma levels of hCRP in hCRP-Tg-1 and hCRP-Tg-2 rabbits were 0.4±0.13 (n=14) and 57.8±20.6 mg/L (n=12), respectively. In addition, hCRP isolated from Tg rabbit plasma exhibited the ability to activate the rabbit complement. To define the role of hCRP in atherosclerosis, we compared the susceptibility of hCRP-Tg rabbits to cholesterol-rich diet-induced aortic and coronary atherosclerosis with that of non-Tg rabbits. After being fed with a cholesterol-rich diet for 16 weeks, Tg and non-Tg rabbits developed similar hypercholesterolemia and lesion sizes in both aortic and coronary arteries. Immunohistochemical staining and Western blotting revealed that hCRP was indeed present in the lesions but did not affect macrophage accumulation and smooth muscle cell proliferation of the lesions.

Conclusions—Neither high nor low plasma concentrations of hCRP affected aortic or coronary atherosclerosis lesion formation in hCRP-Tg rabbits. (***Circulation.* 2009;120:2088-2094.**)

Key Words: atherosclerosis ■ cardiovascular disease ■ coronary disease ■ pathology ■ risk factors

There have been many controversial and contradictory results published on the effects of C-reactive protein (CRP), and a very active debate continues about its role in the pathogenesis of cardiovascular disease (CVD).[1–5] Despite the clinical importance of CRP as a potential marker of increased risk of CVD,[6] the lack of an appropriate animal model has made it difficult to determine whether CRP is merely a marker or is an active mediator in the progression of CVD.[1] Several lines of evidence have revealed that CRP may modulate vascular function, thereby directly participating in the pathogenesis of atherosclerosis.[7,8] This notion has been suggested by the pathological demonstration of CRP in atherosclerotic lesions[9] and the finding that CRP causes a number of biological changes in endothelial cells, smooth muscle cells, and macrophages in vitro that are considered to promote lesion progression.[7] In addition, the recent JUPITER trial (Justification for the Use of Statins in Primary Prevention: an Intervention Trial Evaluating Rosuvastatin) showed that a lipid-lowering drug, rosuvastatin (Crestor), can significantly reduce the incidence of major cardiovascular events even in apparently healthy subjects not exhibiting established risk factors such as hyperlipidemia but with relatively high baseline plasma CRP levels (≥2 mg/L).[10] These studies thus far have raised concerns in regard to whether we should develop CRP-lowering therapies for reducing CVD or whether we should aggressively treat those CVD patients with high levels of CRP in both primary and secondary prevention stages in the same way used to treat hyperlipidemia.[11,12]

Editorial see p 2036
Clinical Perspective on p 2094

Unfortunately, the critical issue of whether high levels of CRP are indeed atherogenic remains unresolved.[3] Many

Received April 12, 2009; accepted September 4, 2009.

From the Departments of Molecular Pathology (T.K., Y.Y., J.Z., J.F.) and Clinical and Laboratory Medicine (Y.O.), Interdisciplinary Graduate School of Medicine and Engineering, University of Yamanashi, Yamanashi, Japan; Analytical Research Center for Experimental Sciences, Saga University, Saga, Japan (S.K., K.N.); Cardiovascular Center, Department of Internal Medicine, University of Michigan, Ann Arbor (J.Z., Y.E.C.); Department of Rehabilitation, Kumamoto Health Science University, Kumamoto, Japan (M.M.); Fukuoka Wajiro Hospital, Fukuoka, Japan (T.W.); Institute of Medical Microbiology and Hygiene, Mainz, Germany (S.B.); and First Department of Pathology, Faculty of Medicine, Miyazaki University, Miyazaki, Japan (Y.A.).

*The first 2 authors contributed equally to this work. †Drs Chen and Fan shared the role of senior author.

The online-only Data Supplement is available with this article at http://circ.ahajournals.org/cgi/content/full/CIRCULATIONAHA.109.872796/DC1.

Correspondence to Dr Jianglin Fan, Department of Molecular Pathology, Interdisciplinary Graduate School of Medicine and Engineering, University of Yamanashi, 1110 Shimokato, Chuo-City, Yamanashi, 409-3898, Japan. E-mail fan_molpatho@yahoo.co.jp

Circulation **is available at http://circ.ahajournals.org** **DOI: 10.1161/CIRCULATIONAHA.109.872796**

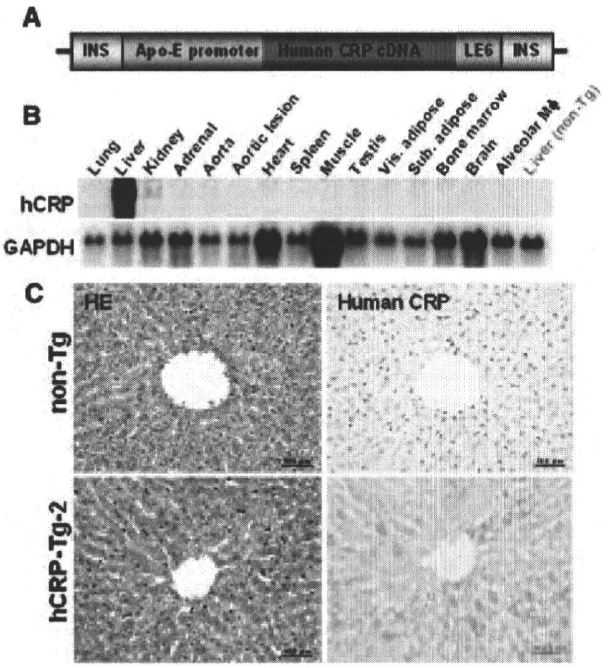

Figure 1. Tg construct for the generation of Tg rabbits (A). The 10.9-kb Tg construct contains the human apolipoprotein E (Apo-E) promoter, hCRP complementary DNA (cDNA), and apolipoprotein E liver element sequences (LE6) with 4 copies of chicken β-globin insulator (INS). Northern blotting was performed to examine the hCRP transgene expression in hCRP-Tg-2 rabbits (B). Hematoxylin-eosin (HE) staining (left) and immunohistochemical staining of the liver with the use of mAb against hCRP (right) are shown in C.

researchers have attempted to address this issue using transgenic (Tg) mice expressing either human CRP (hCRP) or rabbit CRP, but the results thus far are quite controversial and contradictory: CRP is either proatherogenic,[13,14] has no effect on atherosclerosis,[15–19] or is even atheroprotective.[20] Although the cause of these discrepancies is unclear, it appears that the mouse is not an appropriate model for evaluation of CRP because plasma levels of CRP in mice, even in the presence of inflammatory stimuli, are extremely low compared with humans and rabbits.[21] Furthermore, hCRP and rabbit CRP cannot activate complement in the mouse.[17] Given the limitations of the CRP Tg mouse models, it is imperative to develop CRP Tg rabbits as an alternative model for the study of CRP in vivo. Rabbits have been used as an excellent model for human atherosclerosis because their lipoprotein metabolism and cardiovascular system are similar to those of humans.[22] In addition, the acute-phase reactant CRP response of rabbits resembles that of humans more than the mice,[23] and rabbit CRP and hCRP have similar characteristics in structure and function.[24] Furthermore, we have demonstrated that the severity of atherosclerosis is also closely associated with plasma CRP levels in cholesterol-fed and Watanabe heritable hyperlipidemic rabbits.[9] In the present study, we have successfully generated 2 lines of hCRP Tg rabbits and compared the susceptibility of Tg rabbits to cholesterol-rich diet-induced aortic and coronary atherosclerosis with that of non-Tg rabbits.

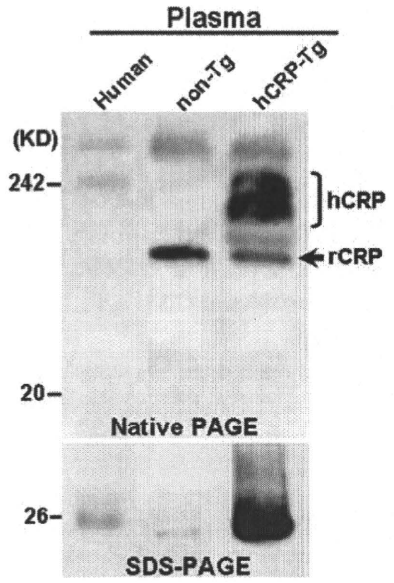

Figure 2. Western blotting analysis of plasma CRP of Tg-2 and non-Tg rabbits by either nondenaturing gel (top) or SDS-PAGE (bottom) and immunoblotted with hCRP mAb as described in Methods. Human plasma obtained from a volunteer was used as a positive control. rCRP indicates rabbit endogenous CRP.

Methods

Generation of Tg Rabbits

Tg rabbits were generated by the methods described previously.[22] In this study, Japanese White rabbits (std:JW/CSK) were purchased from SLC, Inc (Shizuoka, Japan), and zygotes were microinjected with a DNA construct consisting of 1.13 kb hCRP complementary DNA under the control of liver-specific expression elements from the human apolipoprotein E gene[25] with 4 copies of the chicken β-globin insulator (kindly provided by Dr Gary Felsenfeld, National Institutes of Health) (Figure 1A). Insulators can prevent the position effect of transgenes.[26] All animal experiments were performed with the approval of the Animal Care Committee of the universities of Yamanashi and Saga and conformed to the Guide for the Care and Use of Laboratory Animals published by the National Institutes of Health. Two Tg founders were identified by Southern blotting[25] and mated with non-Tg rabbits to produce F1 progeny. To examine the messenger RNA expression of hCRP, total RNA was isolated from various tissues of the Tg rabbits with the use of Trizol reagent (Invitrogen, Life Technologies Inc, Carlsbad, Calif), and Northern blotting was performed as described previously.[27]

Western Blotting and Complement Consumption Assay

hCRP concentrations in the plasma of Tg rabbits were measured by latex agglutination with the use of an automatic analyzer (JCA-BM2250, JEOL, Tokyo, Japan). Two founder Tg rabbits expressed hCRP in the plasma at levels of 0.8 mg/L (designated as Tg-1) and 50 mg/L (designated as Tg-2). To analyze hCRP proteins in Tg rabbit plasma, we subjected the plasma to electrophoresis on a 4% to 12% nondenaturing polyacrylamide gradient gel without sodium dodecyl sulfate (SDS)[28] and also on 10% SDS–polyacrylamide gels (SDS-PAGE), followed by immunoblotting with hCRP monoclonal antibody (mAb). To investigate whether hCRP produced by Tg rabbits was physiologically functional, we isolated hCRP from Tg-2 rabbit plasma using an affinity column with rabbit mAb against hCRP (Epitomics Inc, Burlingame, Calif) and 0.1 mol/L glycine-HCl (pH 2.5) as elution buffer. As described previously,[17] a complement consumption assay was conducted with the use of enzymatically modified human low-density lipoprotein (E-LDL) as a CRP ligand. E-LDL concentrations (400 to 800 μg/mL) were adjusted in accor-

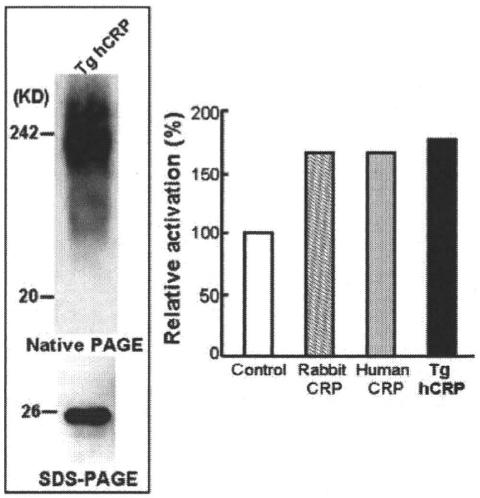

Figure 3. Western blotting analysis and complement activation assay. Tg hCRP was isolated from Tg-2 rabbit plasma as described in Methods and analyzed by either nondenaturing gel (top) or SDS-PAGE (bottom) and immunoblotted with hCRP mAb (left). Isolated Tg hCRP from Tg rabbits exhibited the same ability to augment activation of rabbit serum complement by E-LDL as native rabbit and hCRP (right).

dance with the rabbit sera so that a background consumption of ≈50% was achieved without CRP. The complement consumption induced by E-LDL alone was used as a control and expressed as 100%. Total consumption of CRP from different sources (normal rabbit, human, and Tg-2 rabbit) was compared with that of the controls.

Analysis of Blood and Plasma Biochemistry

To exclude the possibility that expression of hCRP may have any adverse effects on rabbit health, blood cells were analyzed with the use of an automated hematology analyzer (Sysmex XE-2100, Sysmex Co, Kobe, Japan), and plasma biochemistry was measured with the use of an autoanalyzer (JCA-BM2250, JEOL, Tokyo, Japan).

Cholesterol-Rich Diet Experiments

To investigate the effect of hCRP on the development of atherosclerosis, male Tg rabbits (4 to 5 months) and sex- and age-matched non-Tg littermates were fed a diet containing 0.3% cholesterol and 3% soybean oil for 16 weeks. To minimize the variations of plasma cholesterol concentrations in cholesterol-fed rabbits, we measured plasma lipids biweekly and adjusted the cholesterol content of the diet according to the changes in plasma cholesterol of each animal. Hypercholesterolemia of both Tg and non-Tg rabbits was induced and maintained at "atherogenic levels" (600 to 1200 mg/dL) throughout the experiment (see below). The animals were fed ad libitum, and plasma levels of total cholesterol, triglycerides, and high-density lipoprotein cholesterol were measured with the use of Wako assay kits (Wako Pure Chemical Industries, Ltd, Osaka, Japan). Plasma levels of hCRP were measured before and after cholesterol diet feeding for 16 weeks. For the analysis of lipoprotein profiles and apolipoproteins, plasma lipoproteins from rabbits at 8 and 16 weeks of cholesterol diet feeding were isolated by sequential ultracentrifugation and analyzed as described previously.[29]

Quantification of Aortic and Coronary Atherosclerosis

At the end of the cholesterol diet feeding, all rabbits were euthanized by injection of an overdose of sodium pentobarbital solution. The aortas were en face stained with Sudan IV for evaluation of gross atherosclerotic lesions as described previously.[30] For microscopic quantification of lesion areas, each portion of the aorta was dehy-

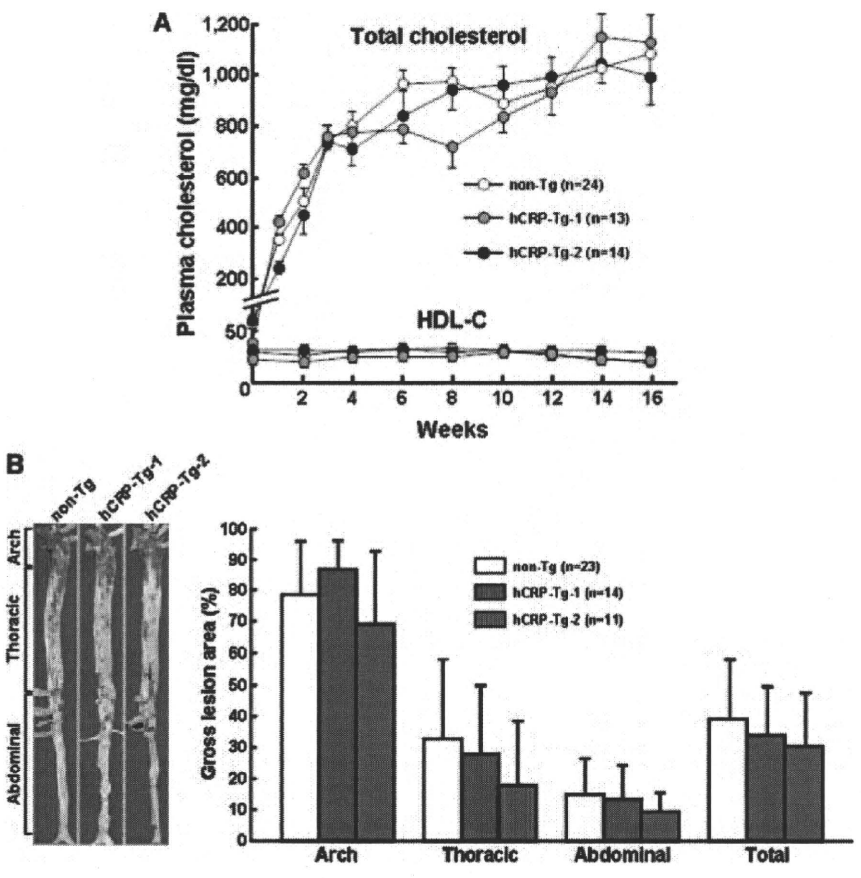

Figure 4. hCRP-Tg rabbits developed hypercholesterolemia similar to that of non-Tg rabbits during cholesterol diet feeding (A, left). The values are expressed as mean±SE. HDL-C indicates high-density lipoprotein cholesterol. Representative photographs of pinned-out aortic trees stained with Sudan IV from each group are shown (B, left), and aortic atherosclerotic lesions (defined by sudanophilic area) on the surface were quantified by an image analysis system (B, right). The values are expressed as mean±SD. $P<0.05$, $P=0.36$, $P=0.52$, and $P=0.49$ in arch, thoracic, abdominal, and whole aorta, respectively, by ANOVA. Because $P<0.05$ by ANOVA was noted in arch, we further analyzed these data by Scheffé F test and found that $P=0.38$ (non-Tg vs Tg-1) and $P=0.35$ (non-Tg vs Tg-2). Therefore, there was no statistical difference between Tg and non-Tg rabbits in all parts of the aorta.

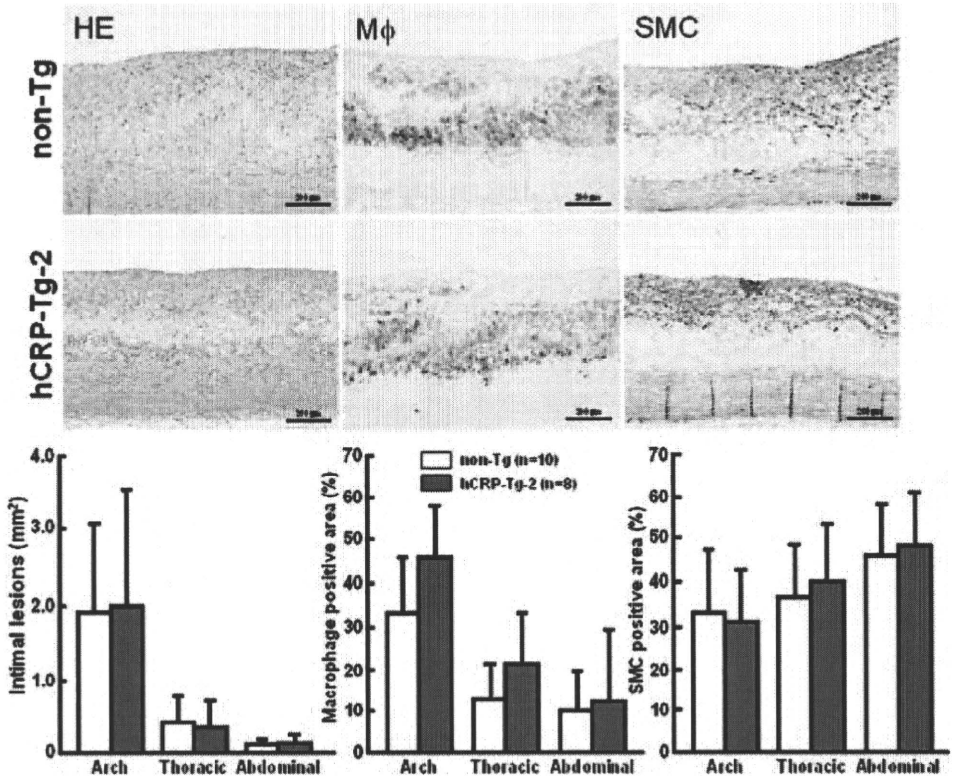

Figure 5. Representative micrographs of the aortic lesions from Tg and non-Tg rabbits (top). Serial paraffin cross sections of aortic lesions were stained with hematoxylin-eosin (HE) or immunohistochemically stained with mAbs against either macrophages (Mφ) or α-smooth muscle actin for smooth muscle cells (SMC). Microscopic analysis of the intimal lesion size and cellular components by immunohistochemical staining is shown (bottom). Intimal lesions on elastica van Gieson–stained sections were quantified with an image analysis system (left). Positively stained areas of immunostained macrophages and smooth muscle cells are quantified (middle and right). The values are expressed as mean±SD. Intimal lesions: $P=0.90$, $P=0.66$, and $P=0.54$ in arch, thoracic, and abdominal aorta, respectively. Mφ-positive area: $P=0.06$, $P=0.10$, and $P=0.76$ in arch, thoracic, and abdominal aorta, respectively. Smooth muscle cell–positive area: $P=0.74$, $P=0.56$, and $P=0.76$, in arch, thoracic, and abdominal aorta, respectively. All comparisons were made by Student's *t* test.

drated in ethanol and embedded in paraffin (10 segments for the aortic arch and abdominal aorta and 20 for the thoracic aorta). All specimens were cut into 3-μm-thick sections and stained with hematoxylin and eosin and elastica van Gieson. For microscopic evaluation of the cellular components of the lesions, serial paraffin-embedded sections of the aorta were immunohistochemically stained with mAbs against macrophages (RAM11) and α-smooth muscle actin (HHF35),[30] as shown in Table I in the online-only Data Supplement, and visualized with Histofine Simple Stain MAX-PO(M) kits (Nichirei Biosciences Inc, Tokyo, Japan). To assess coronary atherosclerosis, rabbit hearts were sectioned into 7 blocks, and the lesions of the left and right coronary arteries were quantified under a light microscope and expressed as the stenosis (%) of the lumen area [lesion area/(total lumen area)×100%] by the method described previously.[30,31] All measurements were performed blindly and independently by 2 separate researchers. To detect CRPs in lesions, immunohistochemical staining was performed with the use of Abs against hCRP and rabbit CRP. We first evaluated the reactivity of 2 Abs against denatured proteins by SDS-PAGE followed by Western blotting and found that hCRP mAb showed slight cross-reactivity with rabbit plasma CRP, whereas rabbit CRP polyclonal Ab cross-reacted with hCRP (Figure I in the online-only Data Supplement). For native CRP (though fixed) in the lesions, hCRP mAb showed slight cross-reactivity with rabbit CRP (see below). Because this cross-reactivity was faint and not often present compared with the reactivity of rabbit CRP Ab in the same section, we could evaluate the hCRP deposition in the lesions by immunohistochemical staining. For negative controls, primary Abs were replaced by either nonspecific mouse immunoglobulin G or chicken immunoglobulin Y. In addition, the lesions of aortas were homogenized, and proteins (10 μg) were run on SDS-PAGE followed by immunoblotting with hCRP mAb.

Statistical Analysis

ANOVA was used to assess differences between 3 groups of gross aortic lesions and plasma biochemistry. Two-factor repeated-measures ANOVA was used for the time-course data of plasma lipids after a cholesterol-rich diet. One-way ANOVA with the Scheffé *F* test or Kruskal-Wallis test was used for parametric and nonparametric analysis. Microscopic analyses of aortic lesions, coronary arterial lesions, and plasma lipoproteins between 2 groups were compared by Student's *t* test or Mann–Whitney *U* test depending on the data distribution. In all cases, statistical significance was set at $P<0.05$.

Results

Characterization of Tg Rabbits

We generated 2 lines of Tg rabbits expressing different levels of plasma hCRP. Average plasma levels of hCRP in F1 Tg-1 and Tg-2 rabbits at 3 to 4 months were 0.4±0.13 (n=14) and 57.8±20.6 mg/L (n=12), respectively (Figure II in the online-only Data Supplement). The hCRP transcripts were expressed almost exclusively in the liver of Tg rabbits (Figure 1B). Histological examination revealed no abnormalities in the liver of Tg rabbits, and hCRP-immunoreactive proteins were immunohistochemically detected only in hepatocytes but not in blood vessels or bile ducts (Figure 1C).

Western blotting analysis revealed that hCRP in the plasma of Tg rabbits was present as a complex with a high molecular weight (pentamer) on nondenaturing gels and a monomer on SDS-PAGE (with an approximate molecular weight of 26 kDa) (Figure 2). To investigate whether hCRP produced by Tg rabbits was physiologically functional, we conducted a complement consumption assay using E-LDL as a CRP ligand. We found that isolated hCRP from Tg-2 rabbis exhibited the same ability to augment activation of rabbit serum complement in the presence of E-LDL as native rabbit and hCRP (Figure 3).

Cholesterol-Rich Diet Experiments

To investigate the effect of hCRP on the development of atherosclerosis, male Tg rabbits and non-Tg littermates were fed a cholesterol-rich diet for 16 weeks. Both Tg and non-Tg rabbits developed similar hypercholesterolemia during the experimental period, and lipoprotein profiles were identical (Figure 4A and Figure III in the online-only Data Supplement). Plasma hCRP levels of Tg-2 rabbits remained as "high" as those of a normal chow diet–fed rabbits during the cholesterol diet, whereas plasma hCRP levels of Tg-1 rabbits were constantly "low" (0.4 to 5 mg/L) (Figure II in the online-only Data Supplement). Expression of hCRP did not lead to obvious changes in the variables of blood and plasma in both Tg rabbits and non-Tg rabbits during the experiment (Table II in the online-only Data Supplement).

Quantification of Aortic and Coronary Atherosclerosis

At the end of the experiment, all rabbits were euthanized, and the severity of aortic and coronary atherosclerosis was examined and quantified with the use of an image analysis system. Compared with non-Tg control rabbits, neither of the Tg rabbit lines showed any statistical differences ($P=0.5$ versus non-Tg by ANOVA) in aortic atherosclerotic lesions defined by Sudan IV staining (Figure 4B). Because plasma levels of hCRP in both lines of Tg rabbits were quite variable at 16 weeks (Figure II in the online-only Data Supplement), we also evaluated the correlation between plasma hCRP and the extent of aortic lesions of each Tg rabbit. However, we did not find any correlations between plasma hCRP and aortic lesions in all Tg rabbits (data not shown). We further examined sections of the lesions under a light microscope and quantified the microscopic lesion areas. However, we did not find any differences in lesion sizes or cellular components (macrophages and smooth muscle cells) between Tg-2 and non-Tg rabbits (Figure 5). To confirm the presence of CRP in lesions, we performed immunohistochemical staining using Abs against either human or rabbit CRP and showed that hCRP-immunoreactive proteins were regularly detected in atherosclerotic lesions of Tg rabbits, whereas rabbit CRP was present in both Tg and non-Tg rabbit lesions (Figure 6, top, and Figure IV in the online-only Data Supplement). Western blotting analysis of the aortic lesions confirmed that the CRP contents were markedly increased in the lesions of Tg rabbits compared with non-Tg rabbits (Figure 6, bottom). Finally, we examined the effect of hCRP on coronary arterial lesions. As shown in Figure 7, the coronary stenosis of Tg-2 rabbits was not statistically different from that of non-Tg rabbits ($P=0.33$ in left and $P=0.64$ in right coronary artery versus non-Tg)

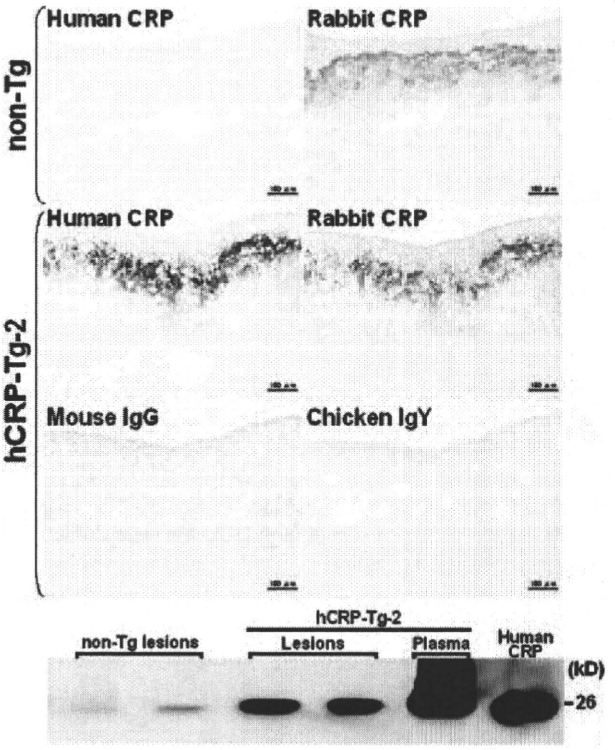

Figure 6. Demonstration of hCRP and rabbit CRP in aortic lesions by immunohistochemical staining (top) and Western blotting analysis (bottom). Human and rabbit CRP-immunoreactive proteins were stained by mouse mAb against hCRP and chicken polyclonal Ab against rabbit CRP, respectively. The negative control staining was performed with the use of mouse nonspecific immunoglobulin G (IgG) and chicken immunoglobulin Y (IgY). hCRP mAb shows slight cross-reaction with rabbit endogenous CRP (top, left). Purified hCRP from Sigma-Aldrich was used as a positive control in Western blotting.

even though CRP-immunoreactive proteins were detected in the lesions. Taken together, hCRP does not affect the development of atherosclerosis in Tg rabbits, which is supported by 2 recent human genetic studies.[32,33]

Discussion

For the first time, we have successfully generated 2 lines of hCRP Tg rabbits to define the role of CRP in atherosclerosis. CRP is a highly controversial marker of CVD. The rabbit model was selected for this undertaking because of its usefulness in studying both the development of atherosclerosis and CRP pathophysiological functions.[22,34]

We found that hCRP isolated from Tg rabbit plasma exhibited the ability to activate the rabbit complement in the presence of E-LDL, confirming that hCRP of Tg rabbits is functional in vivo. Expression of hCRP in Tg rabbits did not lead to any health problems because we did not find any pathological abnormalities, and hematologic and biochemical data of blood were unchanged compared with those of non-Tg rabbits. Spontaneously atherosclerotic lesions were not detected in both lines of hCRP-Tg rabbits on a chow diet for up to 1 year (data not shown). Therefore, we administered a cholesterol-rich diet for 16 weeks, a method that has been used in many studies for investigating the interactions between different genes and the development of atherosclerosis in rabbits.[22] Plasma total choles-

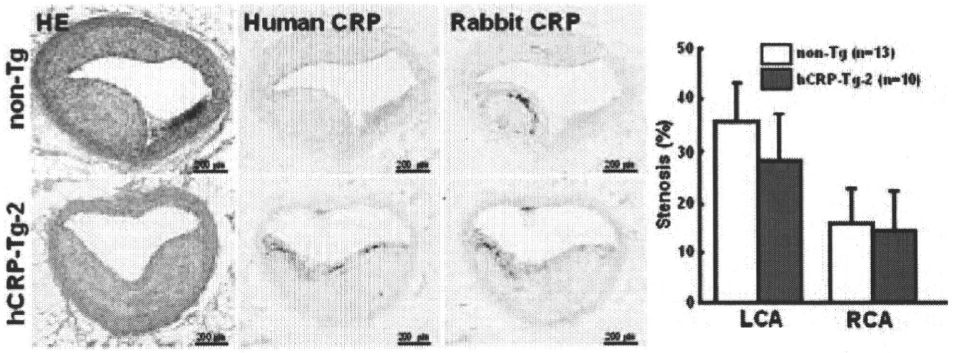

Figure 7. Histological analysis of coronary arterial atherosclerosis and immunodetection of hCRP and rabbit CRP in lesions (left) and quantitatively measured lesion size expressed as stenosis (%) of the lumen area [lesion area/(total lumen area)×100%] (right). HE indicates hematoxylin-eosin. The values are expressed as mean±SE. $P=0.33$ in left coronary artery (LCA) and $P=0.64$ in right coronary artery (RCA) vs non-Tg, analyzed by Mann–Whitney *U* test.

terol levels and lipoprotein profiles of Tg rabbits were basically similar to those of non-Tg rabbits. Taken together, we have established hCRP-Tg rabbits that allow us to investigate the direct effects of plasma hCRP on the development of atherosclerosis.

As illustrated by our analysis, average plasma levels of hCRP-Tg-2 rabbits are above the risk levels (3 to 10 mg/L) generally proposed in humans.[35,36] Plasma hCRP levels of Tg-1 rabbits were initially <1 mg/L but increased to 4.97±4.63 mg/L at 16 weeks of the cholesterol diet. Regardless of hCRP expression in Tg rabbits, both lines of Tg rabbits did not show any enhancement of either lesion size or any changes in the cellular components (macrophages and smooth muscle cells) of lesions. Immunohistochemical staining coupled with Western blotting revealed that hCRP-immunoreactive proteins were indeed present in lesions. Because hCRP, like endogenous rabbit CRP, is expressed exclusively by the liver but not by aorta or macrophages in Tg rabbits, we considered that CRP in the lesions was essentially derived from the circulation rather than synthesized de novo by vascular cells.[34] Despite this observation, both aortic and coronary atherosclerotic lesions were not significantly changed in Tg rabbits compared with non-Tg rabbits, suggesting that hCRP at these levels is not proatherogenic in Tg rabbits. In past years, many studies attempted to demonstrate the atherogenic effect of CRP in genetically modified mice, but the results thus far are controversial.[13,15–17,19,20] It is apparent that our results obtained from 2 lines of Tg rabbits expressing different plasma levels of hCRP rebut the notion that CRP is proatherogenic. Our data are also in support of the recent study showing that genetically elevated CRP does not play a causal role in ischemic vascular disease.[32,33] Nevertheless, we cannot exclude the possibility that hCRP may have a pathophysiological role in aspects of CVD that are not modeled in the present study, such as myocardial infarction[37] and thrombosis.[38] It also remains to be determined whether local CRP present in the arterial wall is involved in plaque rupture. Cross-breeding hCRP Tg rabbits with Watanabe heritable hyperlipidemic myocardial infarction rabbits that develop spontaneous atherosclerosis in both aorta and coronary arteries as well as myocardial infarction[39] will certainly provide a powerful model to examine these hypotheses in the future.

In summary, the present study does not support a direct role of hCRP in the pathogenesis of atherosclerosis in hCRP-Tg rabbits, suggesting that CRP is a marker rather than a maker in the development of atherosclerosis.

Acknowledgments

We thank our students T. Maeda, T. Aoki, and Y. Jin for their help with animal experiments. We also thank K. Sato and M. Ohta, Department of Clinical and Laboratory Medicine, University of Yamanashi Hospital, for analysis of rabbit plasma and blood.

Sources of Funding

This work was supported in part by grants-in-aid for scientific research from the Ministry of Education, Culture, Sports, Science, and Technology, Japan (19390099 and 21659078), a research grant for cardiovascular disease from the Ministry of Health, Labor, and Welfare of Japan, National Institutes of Health grant R01HL088391 (Dr Chen), an American Heart Association National Career Development Grant (0835237N to Dr Zhang), Takeda Science Foundation, ONO Medical Research Foundation, The Naito Foundation, The Uehara Memorial Foundation, Japan Heart Foundation, and a research grant from AstraZeneca. Dr Chen is an established investigator of the American Heart Association (0840025N).

Disclosures

None.

References

1. Nilsson J. CRP: marker or maker of cardiovascular disease? *Arterioscler Thromb Vasc Biol.* 2005;25:1527–1528.
2. Pepys MB, Hirschfield GM. C-reactive protein: a critical update. *J Clin Invest.* 2003;111:1805–1812.
3. Schunkert H, Samani N. Elevated C-reactive protein in atherosclerosis: chicken or egg? *N Engl J Med.* 2008;359:1953–1955.
4. Shah T, Casas JP, Cooper JA, Tzoulaki I, Sofat R, McCormack V, Smeeth L, Deanfield JE, Lowe GD, Rumley A, Fowkes FG, Humphries SE, Hingorani AD. Critical appraisal of CRP measurement for the prediction of coronary heart disease events: new data and systematic review of 31 prospective cohorts. *Int J Epidemiol.* 2009;38:217–231.
5. Casas JP, Shah T, Hingorani AD, Danesh J, Pepys MB. C-reactive protein and coronary heart disease: a critical review. *J Intern Med.* 2008;264:295–314.
6. Ridker PM. C-reactive protein and the prediction of cardiovascular events among those at intermediate risk: moving an inflammatory hypothesis toward consensus. *J Am Coll Cardiol.* 2007;49:2129–2138.
7. Verma S, Devaraj S, Jialal I. Is C-reactive protein an innocent bystander or proatherogenic culprit? C-reactive protein promotes atherothrombosis. *Circulation.* 2006;113:2135–2150.
8. Devaraj S, Singh U, Jialal I. The evolving role of C-reactive protein in atherothrombosis. *Clin Chem.* 2009;55:229–238.
9. Sun H, Koike T, Ichikawa T, Hatakeyama K, Shiomi M, Zhang B, Kitajima S, Morimoto M, Watanabe T, Asada Y, Chen YE, Fan J. C-reactive protein in atherosclerotic lesions: its origin and pathophysiological significance. *Am J Pathol.* 2005;167:1139–1148.

10. Ridker PM, Danielson E, Fonseca F, Genest J, Gotto AJ, Kastelein J, Koenig W, Libby P, Lorenzatti A, MacFadyen J, Nordestgaard B, Shepherd J, Willerson J, Glynn R, Group JS. Rosuvastatin to prevent vascular events in men and women with elevated C-reactive protein. *N Engl J Med.* 2008;359:2195–2207.
11. Jialal I, Devaraj S. Jupiter to earth: CRP promotes atherothrombosis. *Metab Syndr Relat Disord.* 2009;7:1–3.
12. Fuster V, Bansilal S. JUPITER strikes earth. *Nat Clin Pract Cardiovasc Med.* 2009;6:159.
13. Paul A, Ko KW, Li L, Yechoor V, McCrory MA, Szalai AJ, Chan L. C-reactive protein accelerates the progression of atherosclerosis in apolipoprotein E–deficient mice. *Circulation.* 2004;109:647–655.
14. Xing D, Hage FG, Chen YF, McCrory MA, Feng W, Skibinski GA, Majid-Hassan E, Oparil S, Szalai AJ. Exaggerated neointima formation in human C-reactive protein transgenic mice is IgG Fc receptor type I (Fc gamma RI)-dependent. *Am J Pathol.* 2008;172:22–30.
15. Trion A, de Maat MP, Jukema JW, van der Laarse A, Maas MC, Offerman EH, Havekes LM, Szalai AJ, Princen HM, Emeis JJ. No effect of C-reactive protein on early atherosclerosis development in apolipoprotein E*3-leiden/human C-reactive protein transgenic mice. *Arterioscler Thromb Vasc Biol.* 2005;25:1635–1640.
16. Hirschfield GM, Gallimore JR, Kahan MC, Hutchinson WL, Sabin CA, Benson GM, Dhillon AP, Tennent GA, Pepys MB. Transgenic human C-reactive protein is not proatherogenic in apolipoprotein E-deficient mice. *Proc Natl Acad Sci U S A.* 2005;102:8309–8314.
17. Reifenberg K, Lehr HA, Baskal D, Wiese E, Schaefer SC, Black S, Samols D, Torzewski M, Lackner KJ, Husmann M, Blettner M, Bhakdi S. Role of C-reactive protein in atherogenesis: can the apolipoprotein E knockout mouse provide the answer? *Arterioscler Thromb Vasc Biol.* 2005;25:1641–1646.
18. Tennent GA, Hutchinson WL, Kahan MC, Hirschfield GM, Gallimore JR, Lewin J, Sabin CA, Dhillon AP, Pepys MB. Transgenic human CRP is not pro-atherogenic, pro-atherothrombotic or pro-inflammatory in apoE−/− mice. *Atherosclerosis.* 2008;196:248–255.
19. Torzewski M, Reifenberg K, Cheng F, Wiese E, Kupper I, Crain J, Lackner KJ, Bhakdi S. No effect of C-reactive protein on early atherosclerosis in LDLR−/−/human C-reactive protein transgenic mice. *Thromb Haemost.* 2008;99:196–201.
20. Kovacs A, Tornvall P, Nilsson R, Tegner J, Hamsten A, Bjorkegren J. Human C-reactive protein slows atherosclerosis development in a mouse model with human-like hypercholesterolemia. *Proc Natl Acad Sci U S A.* 2007;104:13768–13773.
21. Pepys MB, Baltz M, Gomer K, Davies AJ, Doenhoff M. Serum amyloid P-component is an acute-phase reactant in the mouse. *Nature.* 1979;278:259–261.
22. Fan J, Watanabe T. Transgenic rabbits as therapeutic protein bioreactors and human disease models. *Pharmacol Ther.* 2003;99:261–282.
23. Kushner I, Feldmann G. Control of the acute phase response: demonstration of C-reactive protein synthesis and secretion by hepatocytes during acute inflammation in the rabbit. *J Exp Med.* 1978;148:466–477.
24. Anderson HC, McCarty M. The occurrence in the rabbit of an acute phase protein analogous to human C reactive protein. *J Exp Med.* 1951;93:25–36.
25. Fan J, Wang J, Bensadoun A, Lauer SJ, Dang Q, Mahley RW, Taylor JM. Overexpression of hepatic lipase in transgenic rabbits leads to a marked reduction of plasma high density lipoproteins and intermediate density lipoproteins. *Proc Natl Acad Sci U S A.* 1994;91:8724–8728.
26. Recillas-Targa F, Pikaart MJ, Burgess-Beusse B, Bell AC, Litt MD, West AG, Gaszner M, Felsenfeld G. Position-effect protection and enhancer blocking by the chicken beta-globin insulator are separable activities. *Proc Natl Acad Sci U S A.* 2002;99:6883–6888.
27. Fan J, Unoki H, Kojima N, Sun H, Shimoyamada H, Deng H, Okazaki M, Shikama H, Yamada N, Watanabe T. Overexpression of lipoprotein lipase in transgenic rabbits inhibits diet-induced hypercholesterolemia and atherosclerosis. *J Biol Chem.* 2001;276:40071–40079.
28. Chiesa G, Hobbs HH, Koschinsky ML, Lawn RM, Maika SD, Hammer RE. Reconstitution of lipoprotein(a) by infusion of human low density lipoprotein into transgenic mice expressing human apolipoprotein(a). *J Biol Chem.* 1992;267:24369–24374.
29. Fan J, Ji ZS, Huang Y, de Silva H, Sanan D, Mahley RW, Innerarity TL, Taylor JM. Increased expression of apolipoprotein E in transgenic rabbits results in reduced levels of very low density lipoproteins and an accumulation of low density lipoproteins in plasma. *J Clin Invest.* 1998;101:2151–2164.
30. Liang J, Liu E, Yu Y, Kitajima S, Koike T, Jin Y, Morimoto M, Hatakeyama K, Asada Y, Watanabe T, Sasaguri Y, Watanabe S, Fan J. Macrophage metalloelastase accelerates the progression of atherosclerosis in transgenic rabbits. *Circulation.* 2006;113:1993–2001.
31. Hirata M, Watanabe T. Regression of atherosclerosis in normotensive and hypertensive rabbits: a quantitative analysis of cholesterol-induced aortic and coronary lesions with an image-processing system. *Acta Pathol Jpn.* 1988;38:559–575.
32. Zacho J, Tybjaerg-Hansen A, Jensen JS, Grande P, Sillesen H, Nordestgaard BG. Genetically elevated C-reactive protein and ischemic vascular disease. *N Engl J Med.* 2008;359:1897–1908.
33. Elliott P, Chambers JC, Zhang W, Clarke R, Hopewell JC, Peden JF, Erdmann J, Braund P, Engert JC, Bennett D, Coin L, Ashby D, Tzoulaki I, Brown IJ, Mt-Isa S, McCarthy MI, Peltonen L, Freimer NB, Farrall M, Ruokonen A, Hamsten A, Lim N, Froguel P, Waterworth DM, Vollenweider P, Waeber G, Jarvelin MR, Mooser V, Scott J, Hall AS, Schunkert H, Anand SS, Collins R, Samani NJ, Watkins H, Kooner JS. Genetic loci associated with C-reactive protein levels and risk of coronary heart disease. *JAMA.* 2009;302:37–48.
34. Sun H, Koike T, Ichikawa T, Hatakeyama K, Shiomi M, Zhang B, Kitajima S, Morimoto M, Watanabe T, Asada Y, Chen YE, Fan J. C-reactive protein in atherosclerotic lesions: its origin and pathophysiological significance. *Am J Pathol.* 2005;167:1139–1148.
35. Ridker PM, Rifai N, Rose L, Buring JE, Cook NR. Comparison of C-reactive protein and low-density lipoprotein cholesterol levels in the prediction of first cardiovascular events. *N Engl J Med.* 2002;347:1557–1565.
36. Pearson TA, Mensah GA, Alexander RW, Anderson JL, Cannon RO III, Criqui M, Fadl YY, Fortmann SP, Hong Y, Myers GL, Rifai N, Smith SC Jr, Taubert K, Tracy RP, Vinicor F. Markers of inflammation and cardiovascular disease: application to clinical and public health practice: a statement for healthcare professionals from the Centers for Disease Control and Prevention and the American Heart Association. *Circulation.* 2003;107:499–511.
37. Griselli M, Herbert J, Hutchinson WL, Taylor KM, Sohail M, Krausz T, Pepys MB. C-reactive protein and complement are important mediators of tissue damage in acute myocardial infarction. *J Exp Med.* 1999;190:1733–1740.
38. Danenberg HD, Szalai AJ, Swaminathan RV, Peng L, Chen Z, Seifert P, Fay WP, Simon DI, Edelman ER. Increased thrombosis after arterial injury in human C-reactive protein-transgenic mice. *Circulation.* 2003;108:512–515.
39. Shiomi M, Ito T, Yamada S, Kawashima S, Fan J. Development of an animal model for spontaneous myocardial infarction (WHHLMI rabbits). *Arterioscler Thromb Vasc Biol.* 2003;23:1239–1244.

CLINICAL PERSPECTIVE

Despite the clinical importance of C-reactive protein (CRP) as a potential marker for cardiovascular diseases, the lack of an appropriate animal model has made it difficult to determine whether CRP is merely a marker or is an active mediator in the pathogenesis of atherosclerosis. In past years, studies with the use of transgenic mice expressing either human or rabbit CRP have generated quite controversial and contradictory results. In fact, mice are not appropriate for evaluation of CRP pathophysiology because CRP in mice is not functional in terms of complement activation. In the present study, we have generated novel transgenic rabbits expressing human CRP and documented that human CRP does not affect aortic or coronary atherosclerosis lesion formation in human CRP–transgenic rabbits. Taken together, our data suggest that CRP may not be a contributor of human atherosclerosis.

J. Comp. Path. 2010, Vol. 142, 122–128

Available online at www.sciencedirect.com

ScienceDirect

ELSEVIER
www.elsevier.com/locate/jcpa

A Practical Method for Quantifying Atherosclerotic Lesions in Rabbits

C. Zhang*, H. Zheng*, Q. Yu*, P. Yang*, Y. Li*, F. Cheng*, J. Fan† and E. Liu*

** Laboratory Animal Center, Xi'an Jiaotong University School of Medicine, Xi'an 710061, China and † Department of Molecular Pathology, Interdisciplinary Graduate School of Medicine and Engineering, University of Yamanashi, Yamanashi 409-3898, Japan*

Summary

The rabbit has been widely used for the study of human atherosclerosis; however, the method for analysis of the atherosclerotic lesions has not been standardized between laboratories. The present study reports a practical method for quantifying the changes that occur in aortic atherosclerosis of rabbits. Male Japanese white rabbits were fed with either a standard chow or a diet containing 10% fat and 0.3% cholesterol for 16 weeks. Plasma concentrations of glucose, insulin, total cholesterol, triglycerides and high-density lipoprotein were measured. Aortic atherosclerotic lesions were assessed in quantitative fashion using an image analysis system that measured (1) the gross area of the entire aorta affected by atherosclerosis as defined by Sudan IV staining, (2) the microscopical intimal lesion defined by the elastic van Gieson stain and (3) the infiltration of macrophages and smooth muscle cell proliferation as determined immunohistochemically. The rabbits developed severe aortic atherosclerosis without apparent abnormality of glucose metabolism. The quantitative method described here will be useful for the further investigation of atherosclerosis in rabbits.

Keywords: aorta; atherosclerosis; rabbit

Introduction

The rabbit (*Oryctolagus cuniculus*) is phylogenetically closer to primates than rodents (Graur *et al.*, 1996) and has been used for the investigation of the pathogenesis and treatment of many human diseases including atherosclerosis (Fan *et al.*, 1999; Fan and Watanabe, 2003). Cholesterol-fed rabbits are the most widely employed models for the study of atherosclerosis (Fan and Watanabe, 2000) and the pathology of these experimentally induced lesions resembles that of the spontaneously arising condition in man (Manning *et al.*, 1994; Hong *et al.*, 1997).

The aim of the present study was to determine whether rabbits fed a high fat and high cholesterol diet (HFCD) developed insulin resistance in addition to atherosclerosis. As part of this investigation we present a practical method for the systematic analysis of aortic atherosclerosis in rabbits.

Correspondence to: E. Liu (e-mail: liuenqi@mail.xjtu.edu.cn).

0021-9975/$ - see front matter
doi:10.1016/j.jcpa.2009.08.159

Materials and Methods

Animals and Diets

Japanese white rabbits were provided by the Laboratory Animal Centre of Xi'an Jiaotong University. Twenty male rabbits of approximately 2 kg body weight were randomly divided into two groups fed with either a standard chow diet ($n = 8$) or HFCD ($n = 12$) for 16 weeks. The HFCD was composed of 3.3% corn oil, 6.7% lard and 0.3% cholesterol by weight. Animals were individually maintained in a temperature controlled (20–24°C) facility with a 12 h light/dark cycle, given free access to food and water and acclimatized for 2 weeks before the start of experiment. At the end of the experiment, all rabbits were killed by intravenous injection of an overdose of sodium pentobarbital solution. All animal experiments were approved by the Animal Administration Committee of Xi'an Jiaotong University and performed according to the Xi'an Jiaotong University Guidelines for Animal Experimentation.

Plasma Lipids and Insulin Assay

After 16 h of food deprivation, blood samples were collected via the auricular artery into tubes containing EDTA anticoagulant. Blood samples were stored on ice and centrifuged (950 g, 15 min, 4°C) to obtain plasma. Plasma total cholesterol (TC), triglycerides (TG), glucose and high-density lipoprotein cholesterol (HDL-C) were measured using commercial assay kits (Wako Pure Chemical Industries, Osaka, Japan). The plasma insulin assay was conducted using an enzyme-linked immunoassay kit (Morinaga Bioscience Institute, Yokohama, Japan) with rabbit insulin as a standard.

Glucose Tolerance Test

For the evaluation of glucose metabolism, rabbits were fasted overnight and an intravenous glucose tolerance test (IVGTT) was performed as previously described (Liu *et al.*, 2005). A bolus of glucose (0.6 g/kg body weight) was injected through the ear vein and a blood sample was collected from the auricular artery at 5, 10, 15, 20, 30, 45, 60, 75 and 120 min. Plasma glucose and insulin were assayed as described above. The incremental area under the curve (AUC) was calculated according to the trapezium rule and the insulin resistance index was calculated as previously described (Liu *et al.*, 2005).

Separation of the Arterial Tree

After termination of the experiment, the rabbits were placed in a supine position. A ventral midline incision was made from the mandible to the pelvic area. The common carotid arteries were identified along the ventral surface of the trachea. The muscle of the forelimbs was dissected to expose the right and left subclavian arteries and associated connective tissue. The trachea was carefully cut, raised and lightly elevated together with the common carotid arteries and associated connective tissue containing the subclavian arteries. The arterial tree was then further dissected from other tissue and organs from neck to pelvis. This dissection included the aorta and its branches including the anterior mesenteric artery, the paired renal arteries and the right and left common iliac arteries (Fig. 1). The whole arterial tree was immediately immersed in cold phosphate buffered saline (PBS; pH 7.4, 0.01 M) and kept on ice while periarterial adipose tissue was removed. Finally, the arterial tree was sectioned longitudinally and pinned flat on styrofoam sheets and fixed in 10% neutral buffered formalin for 24 h.

Sudan IV Staining of Arterial Tree

Two dishes containing 70% ethanol and one dish containing 1% Sudan IV solution (10 g Sudan IV dissolved in 1 l of 70% ethanol, mixed overnight at 60°C and filtered) were prepared. The fixed arterial trees were washed in running tap water for 1 h and then immersed with the artery face down in 70% ethanol for 30 min. Subsequently, the arterial trees were placed face down in the Sudan IV solution at room temperature overnight. After staining, the samples were dipped into 70% ethanol for 2–3 min and then placed into a fresh dish of 70% ethanol for 30 min. Finally, the samples were washed in running tap water for 1 h before being stored in 10% neutral buffered formalin. This staining procedure highlighted the atherosclerotic lesions (red) and lesion-free areas of the vessels (white) (Fig. 2A).

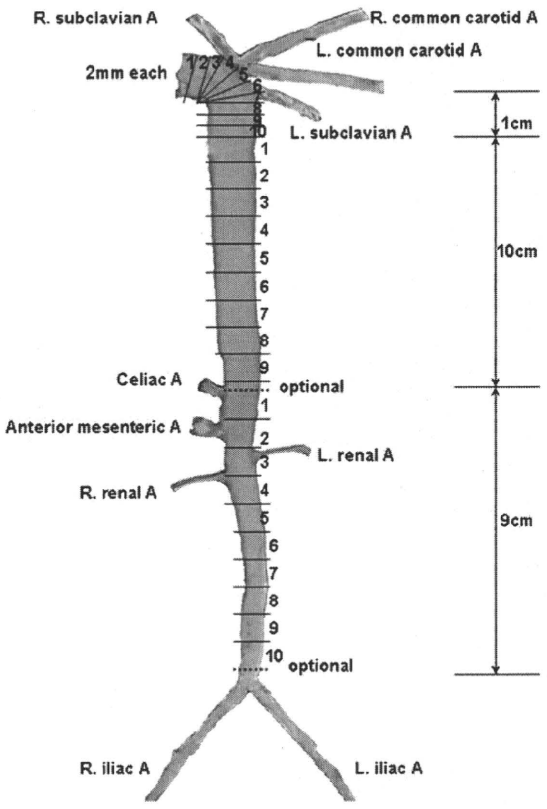

Fig. 1. A schematic illustration of the rabbit arterial tree showing the levels of sectioning applied in the present study. The aorta is considered in three sections: the aortic arch and the thoracic and abdominal aorta. R, right; L, left; A, artery.

Quantification of Gross Lesion Area

The Sudan IV stained arterial trees were photographed for the measurement of the area of gross lesions. The arteries were photographed against a wet dark blue cloth with an adjacent ruler. Digital images were evaluated with Lumina Vision V2.2 image analysis software (Mitani Co., Tokyo, Japan). The aorta was considered in total and as three

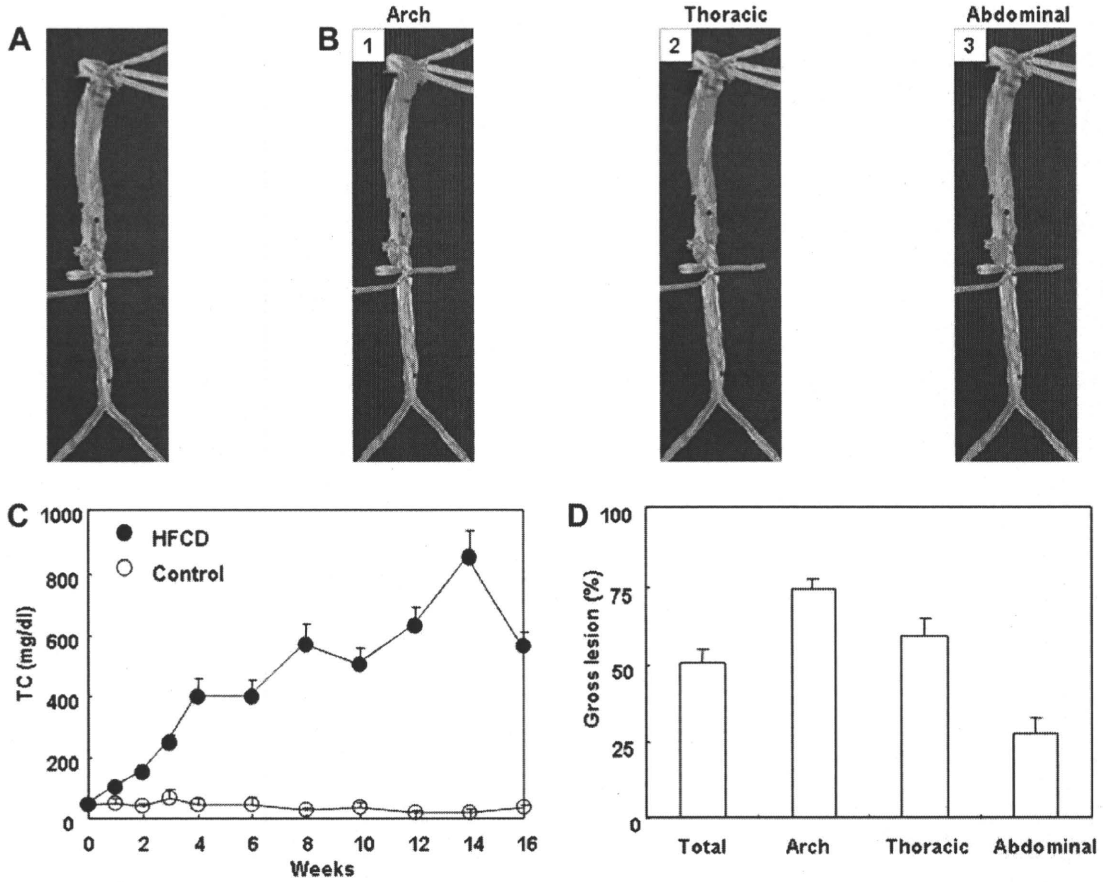

Fig. 2. (A) An arterial tree stained with Sudan IV reveals the distribution of the atherosclerotic lesions in red. (B) The three sections of the aorta defined in Fig. 1 are shown with application of a colour threshold mask to the surface lesions. (C) Plasma total cholesterol (TC) concentration in test and control rabbits for the duration of the experiment shows marked elevation in this parameter in the test animals. (D) Quantitative analysis of the gross lesions of aortic atherosclerosis shows that the most severely affected area of the aorta is the aortic arch.

separate sections: the aortic arch (from the origin at the base of the heart to 1 cm beyond the left subclavian artery), the thoracic (from 1 cm portion beyond the left subclavian artery to the coeliac artery) and the abdominal aorta (from the coeliac artery to the bifurcation of the common iliac arteries). The lesions of aortic atherosclerosis were expressed as the percentage of lesional (Sudanophilic) area relative to the surface area of the entire aorta (Fig. 2B). All measurements were performed independently by two observers unaware of the origin of the vascular trees.

Quantification of Microscopical Lesions

For microscopical examination, the aortic tree was serially sectioned as shown in Fig. 1. The aortic arch (approximately 2 cm long) was sectioned at 2 mm intervals and the thoracic and abdominal aorta was serially sectioned at 1 cm intervals. Representative samples from these sections were processed routinely and embedded longitudinally in paraffin wax. Sections (4 μm) were stained with haematoxylin and eosin (HE) and elastic van Gieson (EVG). EVG stains elastic fibres and therefore highlights the junction between the tunica intima and tunica media. Images of EVG-stained slides were captured with a DP70 digital camera attached to an Olympus BX51 light microscope (Olympus, Tokyo, Japan). The images were analyzed with Lumina Vision V2.2 image analysis software and the intimal lesion size expressed as mm^2 (Fig. 3).

Analysis of Composition of Atherosclerotic Lesions

Immunohistochemistry (IHC) was employed to characterize macrophages (M) (clone RAM11; dilution 1 in 100; DAKO Japan Inc., Tokyo, Japan) and α-smooth muscle actin (SMA; clone HHF35; dilution 1 in 100; Enzo Biochemicals, New York) as previously described (Liang *et al.*, 2006). Briefly, endogenous peroxidase activity was blocked with 3% hydrogen peroxide and then sections were incubated with

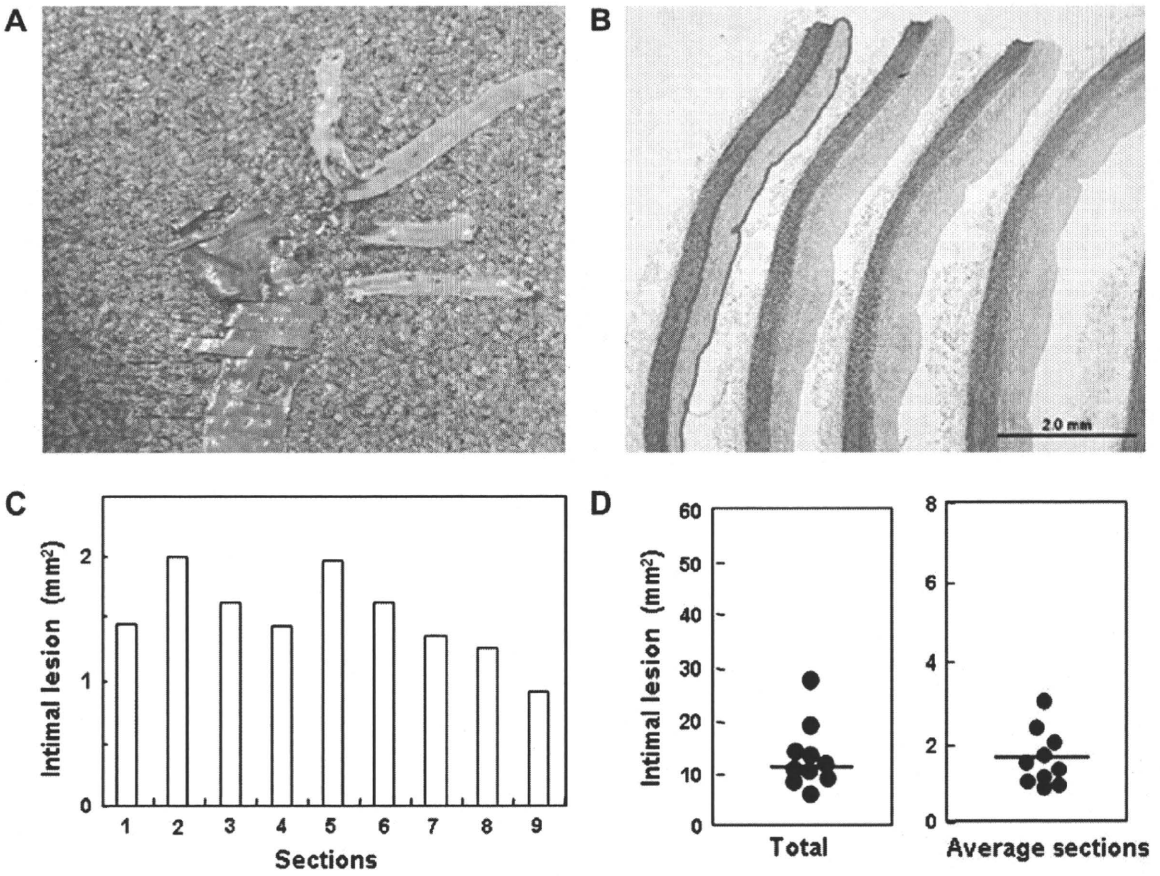

Fig. 3. Microscopical analysis of the intimal lesions. (A) The entire aortic arch was serially sectioned at 2 mm intervals. (B) Longitudinal sections of aortic wall showing delineation of the intima by a traced overlay. (C) The graph presents the intimal lesion area of nine individual sections from the aortic arch of one rabbit. (D) The aortic arch lesion area in HFCD-fed rabbits is shown as total area or average area affected ($n = 10$).

10% normal goat serum to block non-specific binding. The sections were incubated with the primary antibodies at 4°C overnight, followed by 30 min at room temperature with secondary antibody conjugated to horseradish peroxidase (EnVision kit, DAKO). Labelling was 'visualized' with azoethylcarbazol (AEC, Sigma Chemical Company, Japan) and sections were counterstained with Mayer's haematoxylin. The slides were rinsed with PBS between each step. Images of immunolabelled sections were captured with the light microscope camera system described above and analyzed with the same software. Positive labelling (red) was defined by application of a colour threshold mask and the same threshold was applied to all sections. The results are expressed as the percentage of the total lesional area positively labelled for each marker (Fig. 4).

Statistical Analysis

Results were expressed as the mean ± SEM. Statistical analysis was performed using either the Student's *t*-test for data with an equal *F* value or Welch's *t*-test when the *F* value was not equal. $P < 0.05$ was considered statistically significant.

Results

Biochemical Parameters

HFCD feeding resulted in marked increases in plasma concentrations of TG, HDL-C and glucose ($P < 0.01$, Table 1). Plasma TC concentrations in HFCD-fed rabbits were higher than in controls for the duration of the experiment ($P < 0.01$, Fig. 2C). The plasma insulin concentration did not differ between test and control rabbits ($P > 0.05$). There was no significant difference in the AUC of plasma glucose and insulin and the insulin resistance index between the two groups (data not shown).

Gross Atherosclerotic Lesions

The atherosclerotic lesions stained red with Sudan IV (Fig. 2). The ratio of the area of the atherosclerotic lesion relative to that of the entire aorta (51%), the

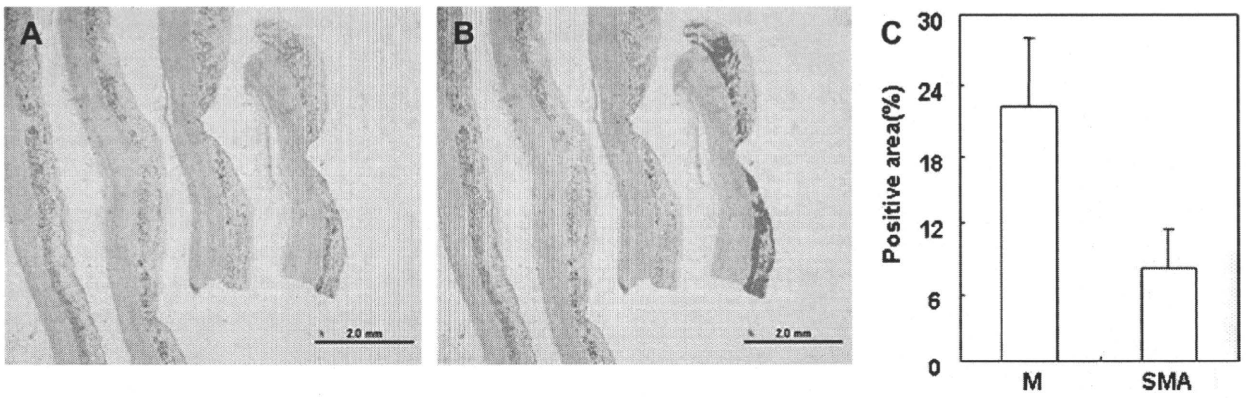

Fig. 4. Microscopical analysis of the distribution of macrophages and α-smooth muscle actin (SMA) within the atherosclerotic lesions. (A) Aortic sections immunohistochemically labelled to show the presence of macrophages. (B) A colour threshold mask is applied to delineate the location of the macrophages. (C) The percentage area occupied by macrophages (M) and SMA is summarized in this histogram.

aortic arch (74%) and the thoracic (60%) and the abdominal (27%) aorta is shown in Fig. 2D. Atherosclerosis was most severe within the aortic arch, followed by the thoracic and abdominal aorta. No atherosclerotic lesions were found in control rabbits.

Quantification of Microscopical Lesions

Microscopical lesions were evaluated in sections from the aortic arch (Figs. 3–5). In HFCD-fed rabbits, the mean total intimal lesion area was 13.01 ± 1.97 mm^2 and the average lesion area of individual sections was 1.59 ± 0.23 mm^2 (Fig. 3). The area of the atherosclerotic lesions occupied by macrophages (22%) and SMA (8%) is shown in Fig. 4.

Discussion

The lipoprotein metabolism of rabbits more closely approximates that of man than does the lipoprotein metabolism of mice. Rabbit and human lipoprotein profiles are rich in low-density lipoproteins (LDL), whereas the lipoprotein profile of the mouse is enriched for high-density lipoproteins (HDL). Rabbits and man have abundant plasma cholesteryl ester transfer protein (CETP), whereas mice are deficient in this molecule. Therefore, rabbits are susceptible to cholesterol-rich diet-induced atherosclerosis, whereas most strains of mice do not develop atherosclerosis after feeding such diets. The rabbit thus provides an appropriate model for investigations of complex diseases such as atherosclerosis, obesity and diabetes mellitus (Fan and Watanabe, 2003; Liu and Fan, 2003).

In those strains of mice that do develop atherosclerotic lesions, various methods have been employed to quantify the extent of the pathology (Paigen *et al.*, 1987; Palinski *et al.*, 1994). The method of dissecting the arterial tree is similar to that described for the rabbit in the present study, but in mice it is more difficult to separate the common carotid and iliac arteries and a dissecting microscope must be used. Because of these technical challenges, murine studies generally involve quantification of atherosclerotic lesions in either specific regions or the aortic root (Daugherty and Whitman, 2003; Baglione and Smith, 2006).

Methods for quantification of atherosclerotic lesions in the rabbit aorta were introduced by Dabanoğlu (2000) and Blümel *et al.* (2001). These authors measured the thickness of the intima, media and adventitia in specific aortic segments or measured gross lesions, but they did not provide a method to evaluate the atherosclerosis lesions overall. The present study provides the first description of a method for dissection of the rabbit arterial tree and for systematic analysis of three aspects of the lesions: (1) the gross lesional area of the entire aorta, (2) the microscopical measurement of the size of intimal lesions and (3) immunohistochemical quantification of key cellular components in the

Table 1
Plasma biochemical parameters after feeding HFCD or normal diet for 16 weeks

Group	*HDL-C (mg/dl)*	*Glucose (mg/dl)*	*Triglycerides (mg/dl)*	*Insulin (ng/ml)*
Control ($n = 8$)	16.39 ± 1.39	111.07 ± 6.06	56.38 ± 3.50	0.67 ± 0.14
HFCD ($n = 10$–12)	165.74 ± 13.95**	137.00 ± 5.44**	87.63 ± 9.28**	0.72 ± 0.05

Data are expressed as mean ± SEM; **, $p < 0.01$ versus control.

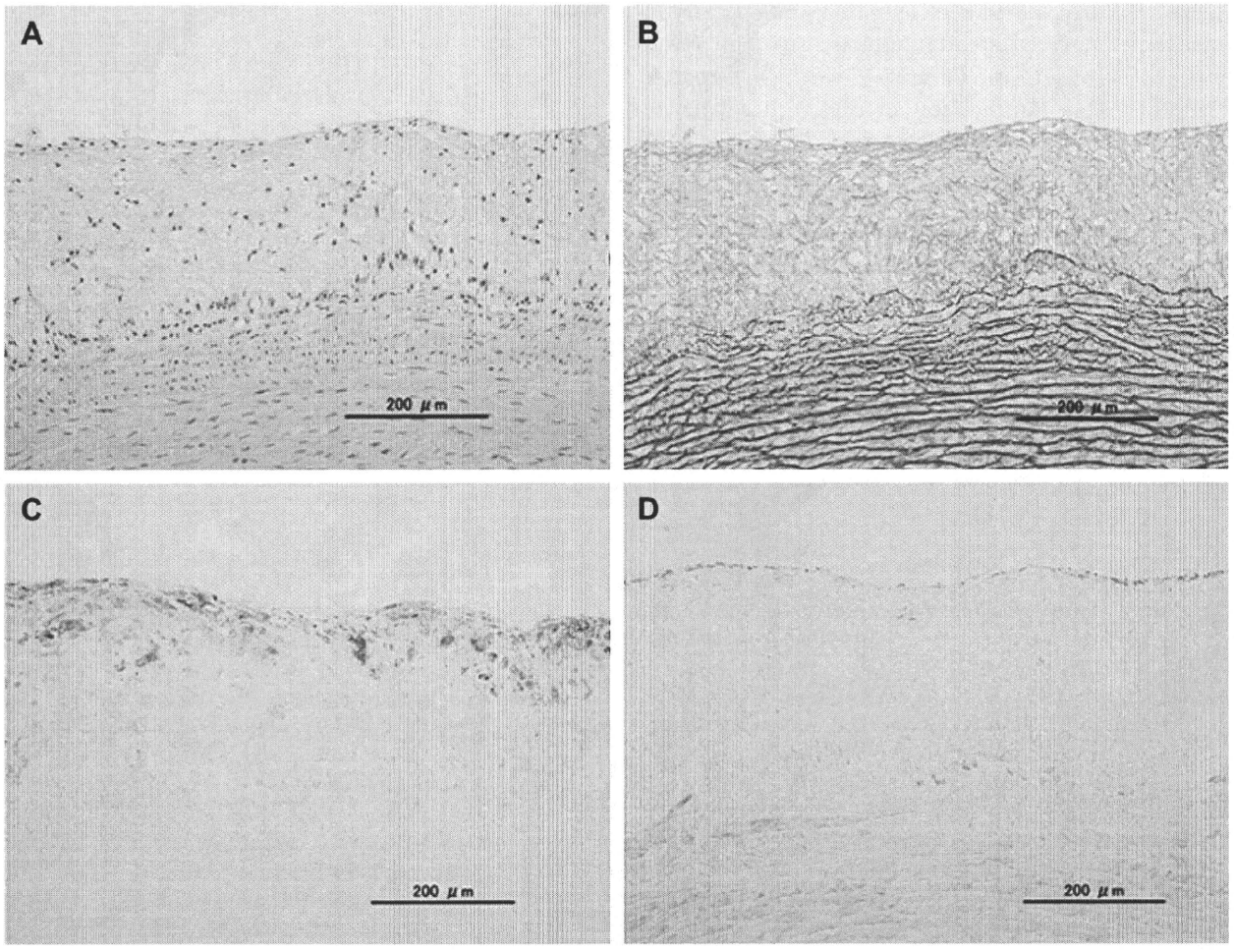

Fig. 5. Representative photomicrographs showing the intimal lesions and cellular components. Serial sections were taken at the aortic arch at the same position and stained with (A) HE and (B) EVG. Immunohistochemical labelling was employed to identify (C) macrophages and (D) α-smooth muscle actin. The intima of the artery is thickened (A, B) and the lesions are seen to comprise layers of foamy macrophages (C) and smooth muscle cells (D) with scattered collections of extracellular lipid droplets (A, B) and particles that disrupt the coherence of some intimal smooth muscle cells (D).

atherosclerotic lesions. In the present study we chose to analyze the distribution of macrophages and SMA in the lesions; however, other cellular components such as extracellular matrix and lipoproteins (Ichikawa *et al.*, 2002) or lipoprotein lipase (Ichikawa *et al.*, 2005) may also be evaluated. In addition, the lesions may be classified (e.g. early stage type I and II lesions or advanced type III–V lesions) according to the criteria of the American Heart Association (Fan *et al.*, 2001; Koike *et al.*, 2005).

The nature of coronary atherosclerotic lesions in rabbits can also be measured. The epicardial branches of the coronary arteries in rabbits have two patterns of distribution, namely bifurcation or trifurcation of the arteria coronaria sinistra (Podesser *et al.*, 1997). Based on this coronary artery anatomy and previous methods, our laboratory has reported a new method for sectioning the entire rabbit heart into seven blocks for examination of the branches of the left and right coronary arteries. These tissue blocks are embedded in paraffin wax and sections are stained with HE and EVG or evaluated immunohistochemically. The lesions of coronary atherosclerosis were quantified and expressed as (1) the intimal lesion area (mm^2), (2) the degree of stenosis (% lesion area/coronary lumen area) and (3) the proportion of the lesion comprised of particular cellular components (% positive area/lesion area) (Liang *et al.*, 2006; Kitajima *et al.*, 2007). In addition, molecular studies of gene expression within such lesions have been reported and the expression of encoded proteins may be evaluated by western blotting (Sun *et al.*, 2005).

The present study attempted to develop a model for the study of insulin resistance and its complications by HFCD manipulation in rabbits. However, the HFCD-fed rabbits did not show insulin resistance or other

related features, but did develop hypercholesterolaemia, hypertriglyceridaemia and extensive and severe aortic atherosclerosis. Therefore, we have reported a method of quantification of such atherosclerotic lesions based on similar studies performed in our laboratory over a number of years (Liang *et al.*, 2006; Kitajima *et al.*, 2007; Zhao *et al.*, 2008). The method is simple and accurate and may be applied to studies following the development of the atherosclerotic lesion or to investigations that examine the pathogenesis of atherosclerosis in transgenic models. Current murine studies are investigating the application of high-resolution 3D magnetic resonance imaging to the quantification of atherosclerotic lesions (McAteer *et al.*, 2004). It is hoped that such investigations will enhance our understanding of human atherosclerosis.

References

Baglione J, Smith JD (2006) Quantitative assay for mouse atherosclerosis in the aortic root. *Methods in Molecular Medicine*, **129**, 83–95.

Blümel JE, Castelo-Branco C, Sanjuán A, González P, Moyano C *et al.* (2001) A simplified method to quantitate atherosclerosis in the rabbit aorta. *Maturitas*, **39**, 265–271.

Dabanoğlu I (2000) A quantitative study of the aorta of the New Zealand rabbit (*Oryctolagus cuniculus*). *Anatomia, Histologia, Embryologia*, **29**, 145–147.

Daugherty A, Whitman SC (2003) Quantification of atherosclerosis in mice. *Methods in Molecular Biology*, **209**, 293–309.

Fan J, Challah M, Watanabe T (1999) Transgenic rabbit models for biomedical research: current status, basic methods and future perspectives. *Pathology International*, **49**, 583–594.

Fan J, Shimoyamada H, Sun H, Marcovina S, Honda K *et al.* (2001) Transgenic rabbits expressing human apolipoprotein (a) develop more extensive atherosclerotic lesions in response to a cholesterol-rich diet. *Arteriosclerosis, Thrombosis and Vascular Biology*, **21**, 88–94.

Fan J, Watanabe T (2000) Cholesterol-fed and transgenic rabbits for the study of atherosclerosis. *Journal of Atherosclerosis and Thrombosis*, **7**, 26–32.

Fan J, Watanabe T (2003) Transgenic rabbits as therapeutic protein bioreactors and human disease models. *Pharmacology and Therapeutics*, **99**, 261–282.

Graur D, Duret L, Gouy M (1996) Phylogenetic position of the order Lagomorpha (rabbits, hares and allies). *Nature*, **379**, 333–335.

Hong MK, Vossoughi J, Mintz GS, Kauffman RD, Hoyt RF *et al.* (1997) Altered compliance and residual strain precede angiographically detectable early atherosclerosis in low-density lipoprotein receptor deficiency. *Arteriosclerosis, Thrombosis and Vascular Biology*, **17**, 2209–2217.

Ichikawa T, Liang J, Kitajima S, Koike T, Wang X *et al.* (2005) Macrophage-derived lipoprotein lipase increases aortic atherosclerosis in cholesterol-fed Tg rabbits. *Atherosclerosis*, **179**, 87–95.

Ichikawa T, Unoki H, Sun H, Shimoyamada H, Marcovina S *et al.* (2002) Lipoprotein (a) promotes smooth muscle cell proliferation and dedifferentiation in atherosclerotic lesions of human apo (a) transgenic rabbits. *American Journal of Pathology*, **160**, 227–236.

Kitajima S, Jin Y, Koike T, Yu Y, Liu E *et al.* (2007) Lp (a) enhances coronary atherosclerosis in transgenic Watanabe heritable hyperlipidemic rabbits. *Atherosclerosis*, **193**, 269–276.

Koike T, Liang J, Wang X, Ichikawa T, Shiomi M *et al.* (2005) Enhanced aortic atherosclerosis in transgenic Watanabe heritable hyperlipidemic rabbits expressing lipoprotein lipase. *Cardiovascular Research*, **65**, 524–534.

Liang J, Liu E, Yu Y, Kitajima S, Koike T *et al.* (2006) Macrophage metalloelastase accelerates the progression of atherosclerosis in transgenic rabbits. *Circulation*, **113**, 1993–2001.

Liu E, Fan J (2003) Transgenic rabbit models for the study of atherosclerosis: current status and future perspectives. *Chinese Journal of Arteriosclerosis*, **11**, 371–375.

Liu E, Kitajima S, Higaki Y, Morimoto M, Sun H *et al.* (2005) High lipoprotein lipase activity increases insulin sensitivity in transgenic rabbits. *Metabolism*, **54**, 132–138.

Manning PJ, Ringler DH, Newcomer CE (1994) *The Biology of the Laboratory Rabbit*. 2nd Edit., Academic Press, San Diego. pp. 367–375.

McAteer MA, Schneider JE, Clarke K, Neubauer S, Channon KM *et al.* (2004) Quantification and 3D reconstruction of atherosclerotic plaque components in apolipoprotein E knockout mice using ex vivo high-resolution MRI. *Arteriosclerosis, Thrombosis and Vascular Biology*, **24**, 2384–2390.

Paigen B, Morrow A, Holmes PA, Mitchell D, Williams RA (1987) Quantitative assessment of atherosclerotic lesions in mice. *Atherosclerosis*, **68**, 231–240.

Palinski W, Ord VA, Plump AS, Breslow JL, Steinberg D *et al.* (1994) ApoE-deficient mice are a model of lipoprotein oxidation in atherogenesis. Demonstration of oxidation-specific epitopes in lesions and high titers of autoantibodies to malondialdehyde-lysine in serum. *Arteriosclerosis, Thrombosis and Vascular Biology*, **14**, 605–616.

Podesser B, Wollenek G, Seitelberger R, Siegel H, Wolner E *et al.* (1997) Epicardial branches of the coronary arteries and their distribution in the rabbit heart: the rabbit heart as a model of regional ischemia. *Anatomical Record*, **247**, 521–527.

Sun H, Koike T, Ichikawa T, Hatakeyama K, Shiomi M *et al.* (2005) C-reactive protein in atherosclerotic lesions: its origin and pathophysiological significance. *American Journal of Pathology*, **167**, 1139–1148.

Zhao S, Zhang C, Lin Y, Yang P, Yu Q *et al.* (2008) The effects of rosiglitazone on aortic atherosclerosis of cholesterol-fed rabbits. *Thrombosis Research*, **123**, 281–287.

[*Received, March 27th, 2009*
Accepted, August 27th, 2009]

Eur J Nucl Med Mol Imaging (2010) 37:2093–2104
DOI 10.1007/s00259-010-1521-2

ORIGINAL ARTICLE

Imaging with radiolabelled anti-membrane type 1 matrix metalloproteinase (MT1-MMP) antibody: potentials for characterizing atherosclerotic plaques

Yuji Kuge · Nozomi Takai · Yuki Ogawa · Takashi Temma · Yan Zhao · Kantaro Nishigori · Seigo Ishino · Junko Kamihashi · Yasushi Kiyono · Masashi Shiomi · Hideo Saji

Received: 17 December 2009 / Accepted: 3 June 2010 / Published online: 13 July 2010

Abstract
Purpose Membrane type 1 matrix metalloproteinase (MT1-MMP) activates pro-MMP-2 and pro-MMP-13 to their active forms and plays important roles in the destabilization of atherosclerotic plaques. This study sought to determine the usefulness of ^{99m}Tc-labelled monoclonal antibody (mAb), recognizing MT1-MMP, for imaging atherosclerosis in a rabbit model (WHHLMI rabbits).
Methods Anti-MT1-MMP monoclonal IgG_3 and negative control IgG_3 were radiolabelled with ^{99m}Tc after derivatization with 6-hydrazinonicotinic acid (HYNIC) to yield ^{99m}Tc-MT1-MMP mAb and ^{99m}Tc-IgG_3, respectively. WHHLMI and control rabbits were injected with these radio-probes. The aorta was removed and radioactivity was measured at 24 h after the injection. Autoradiography and histological studies were performed.
Results ^{99m}Tc-MT1-MMP mAb accumulation in WHHLMI rabbit aortas was 5.4-fold higher than that of control rabbits. Regional ^{99m}Tc-MT1-MMP mAb accumulation was positively correlated with MT1-MMP expression (r=0.59, p<0.0001), while ^{99m}Tc-IgG_3 accumulation was independent of MT1-MMP expression (r=0.03, p=NS). The highest ^{99m}Tc-MT1-MMP mAb accumulation was found in atheromatous lesions (4.8±1.9, %ID×BW/mm^2×10^2), followed in decreasing order by fibroatheromatous (1.8±1.3), collagen-rich (1.6±1.0) and neointimal lesions (1.5±1.5). In contrast, ^{99m}Tc-IgG_3 accumulation was almost independent of the histological grade of lesions.
Conclusion Higher ^{99m}Tc-MT1-MMP mAb accumulation in grade IV atheroma was shown in comparison with neointimal lesions or other more stable lesions. Nuclear imaging with ^{99m}Tc-MT1-MMP mAb, in combination with CT and MRI, could provide new diagnostic imaging capabilities for detecting vulnerable plaques, although further investigations to improve target to blood ratios are strongly required.

Keywords Atherosclerosis · Imaging · Matrix metalloproteinase · Antibody · Rabbit

Y. Kuge · N. Takai · Y. Ogawa · T. Temma · K. Nishigori · S. Ishino · J. Kamihashi · Y. Kiyono · H. Saji
Department of Patho-functional Bioanalysis, Graduate School of Pharmaceutical Sciences, Kyoto University, Kyoto, Japan

Y. Kuge · Y. Zhao
Department of Tracer Kinetics & Bioanalysis, Graduate School of Medicine, Hokkaido University, Sapporo, Japan

Y. Kuge (✉)
Central Institute of Isotope Science, Hokkaido University, Kita 15 Nishi 7, Kita-ku, Sapporo 060-0815, Japan
e-mail: kuge@ric.hokudai.ac.jp

Y. Kiyono
Biomedical Imaging Research Center, University of Fukui, Fukui, Japan

M. Shiomi
Institute for Experimental Animals, Kobe University Graduate School of Medicine, Kobe, Japan

Introduction

Since the rupture of atherosclerotic plaques and subsequent thrombus formation are the major causes of ischaemic diseases, such as cerebral and myocardial infarctions [1–3],

the detection of atherosclerotic plaques at higher risk for rupture is clinically important for early selection and administration of appropriate therapy. There are several techniques for imaging atherosclerotic plaques, such as computed tomography (CT), magnetic resonance imaging (MRI), ultrasound (US) and intravascular ultrasound (IVUS). These non-invasive anatomical imaging modalities offer excellent resolution and visualize the arterial lumen or calcifications. These modalities can identify the morphological alteration of atherosclerotic plaque and play important roles in finding the patients whose lesion vulnerability needs to be further evaluated. To date, however, there are no non-invasive diagnostic tools available for routine clinical use to accurately characterize atherosclerotic plaques at higher risk of rupture. Accordingly, the development of such non-invasive tools is urgently required. Using specific radio-probes, it may be possible for nuclear imaging to characterize atherosclerotic plaques as quantitative images based on cellular and biological changes, which surpasses morphological information and may help selectively detect atherosclerotic plaques at higher risk of rupture [4, 5]. Thus, the development of radio-probes is of great concern in the clinical diagnosis of atherosclerosis.

Plaques that are prone to rupture are morphologically characterized by a thin fibrous cap overlying a large lipid core. Matrix metalloproteinases (MMPs) degrade extracellular matrix that constitutes the fibrous cap of the plaques, resulting in destabilization of atherosclerotic plaques [6–8]. Increased expression of MMP-2 and MMP-9 has been demonstrated within human atherosclerotic lesions and critically implicated in plaque rupture [7, 9, 10]. MMP-2 and MMP-9 are known to cleave native type IV, V, VII and X collagens and elastin, as well as the degradation products of collagens types I, II and III after proteolysis by collagenases, such as MMP-1 and MMP-13. Thus, MMPs are considered to be involved in plaque instability [8] and are potential targets for diagnostic imaging of atherosclerotic plaques at higher risk of rupture [11, 12]. MMPs can be divided into two groups: soluble MMPs and membrane-bound MMPs. Most soluble MMPs, including MMP-2 and MMP-9, are released from cells as zymogens and require extracellular post-translational cleavage to gain biological activity [8, 13]. A membrane-bound MMP, membrane type 1 matrix metalloproteinase (MT1-MMP or MMP-14), mediates activation of pro-MMP-2 to active MMP-2 and pro-MMP-13 to active MMP-13 on the cell surface [13–15]. In our recent animal study, co-distribution of MT1-MMP and MMP-2 was demonstrated in grade IV atheroma, indicating a possible role for MT1-MMP in destabilization of atherosclerotic plaques [16]. Expression of MT1-MMP has also been found within human atherosclerotic plaques [17, 18]. Accordingly, MT1-MMP may be an important determinant of destabilization of atherosclerotic plaques and detection of MT1-MMP expression may be useful for the assessment of atherosclerotic plaques.

Taken together, nuclear imaging of MT1-MMP could provide molecular and cellular information concerning the destabilization of atherosclerotic plaques. Thus, we designed and prepared ^{99m}Tc-labelled anti-MT1-MMP monoclonal IgG (^{99m}Tc-MT1-MMP mAb) as a radio-probe for imaging atherosclerosis. Using an atherosclerosis model (myocardial infarction-prone Watanabe heritable hyperlipidaemic rabbits, WHHLMI rabbits) [19], we investigated accumulation of ^{99m}Tc-MT1-MMP mAb in atherosclerotic lesions in comparison with histological characteristics. From the data, the potential of ^{99m}Tc-MT1-MMP mAb for imaging atherosclerosis was evaluated.

Materials and methods

Design and preparation of ^{99m}Tc-MT1-MMP mAb

A purified mouse monoclonal antibody (mAb) to an oligopeptide (residues 319 to 333, numbered from the signal peptide) on human MT1-MMP (113-5B7, mouse IgG3, Daiichi Fine Chemical Co., Ltd., Toyama, Japan) [14] was used. For the control study, negative control mouse IgG_3 (ab18392, Abcam, Cambridge, UK) was used.

The anti-MT1-MMP monoclonal IgG_3 (MT1-MMP mAb) and negative control IgG_3 (IgG_3) were radiolabelled with ^{99m}Tc (^{99m}Tc-MT1-MMP mAb and ^{99m}Tc-IgG_3, respectively) after derivatization with 6-hydrazinonicotinic acid (HYNIC), according to the procedures reported previously [20–22] with slight modifications. Briefly, HYNIC-*N*-hydroxysuccinimide (NHS) was reacted with MT1-MMP mAb and IgG_3 to obtain precursors for radiolabelling (HYNIC-MT1-MMP mAb and HYNIC-IgG_3, respectively) and then purified by diafiltration. HYNIC-NHS (25 μl, 5 mg/ml) in dry *N*,*N*-dimethylformamide (DMF) was added to MT1-MMP mAb and IgG_3 solutions in 0.15 M borate buffer (pH 8.5, 2 mg/400 μl), respectively. After gentle stirring with protection from light for 2 h at room temperature, size-exclusion (SE) filtration with a diafiltration membrane [Amicon Ultra-4 (MWCO 30,000), Millipore Co., Billerica, MA, USA] using 0.01 M citrate buffer (pH 5.2) was performed to remove aggregated protein and to obtain HYNIC-MT1-MMP mAb and HYNIC-IgG_3. The purified HYNIC-MT1-MMP mAb and HYNIC-IgG_3 were stored at 4°C and used for the subsequent radiolabelling.

Radiolabelling was performed just before each experiment. To the purified HYNIC-MT1-MMP mAb and HYNIC-IgG_3 solutions (300 μg/500 μl), an equal volume of [^{99m}Tc](tricine)$_2$, prepared by the method of Larsen et al. [23], was added to obtain ^{99m}Tc-MT1-MMP mAb and

^{99m}Tc-IgG$_3$ {[^{99m}Tc](HYNIC-anti-MT1-MMP)(tricine)$_2$ and [^{99m}Tc](HYNIC-IgG$_3$)(tricine)$_2$, respectively}. After 3 h at room temperature, the radiolabelled products were purified by SE chromatography on a PD-10 desalting column (Amersham Biosciences AB, Uppsala, Sweden) using 0.05 M phosphate-buffered saline (PBS) (pH 7.0). The radiochemical purities of ^{99m}Tc-MT1-MMP mAb and ^{99m}Tc-IgG$_3$ were determined by another SE column filtration (PD-10 column) in each preparation and found to be 92.3±1.5% and 92.3±5.5%, respectively.

Animals

Three male Japanese White (JW) rabbits (3 months old, Biotek Inc., Saga, Japan) were used to obtain peritoneal macrophages. For non-invasive imaging and biodistribution studies of ^{99m}Tc-MT1-MMP mAb, four male WHHLMI rabbits (11–18 months old: 3.4±0.4 kg body weight) that were bred at Kobe University were used. Four JW rabbits (3 months old: 2.2±0.1 kg body weight, Biotek Inc., Saga, Japan) were used as controls. Four WHHLMI rabbits (two male and two female, 10–15 months old, 2.9±0.3 kg) were used for non-invasive imaging and biodistribution studies of ^{99m}Tc-IgG$_3$. The animals were fed standard chow (type CR-3, Clea Japan Inc., Tokyo, Japan) at 120 g/day and were given water ad libitum. All animal procedures were approved by the Kyoto University Animal Care Committee.

Immunoreactivity of HYNIC-MT1-MMP mAb

Rabbit peritoneal macrophages were obtained by the method of Ishii et al. [24], with minor modifications. The cells were suspended in medium A [Dulbecco's modified Eagle's medium containing 1 mM glutamine, penicillin (100 U/ml), streptomycin (100 μg/ml) and 0.2% lactalbumin hydrolysate] at a final concentration of 2.5×10^6 cells/ml. Aliquots of the cell suspension were placed into plastic Petri dishes and cultured in a humidified 5% CO_2 incubator at 37°C. After 2 h, each dish was washed twice with medium A and then cultured for a further 18 h. Cells (1×10^6 cells) were incubated with MT1-MMP mAb (50 μg/ml, 100 μl), HYNIC-MT1-MMP mAb (50 μg/ml, 100 μl) or control mouse IgG$_3$ (50 μg/ml, 100 μl) for 30 min at 4°C, followed by incubation with 10 μg/ml of Alexa Fluor® 488 goat anti-mouse IgG (100 μl, Molecular Probes, Inc., Eugene, OR, USA). For flow cytometry analysis, cells were mixed with IsoFlow solution (Beckman Coulter Inc., Fullerton, CA, USA) and immediately analysed by a FACScan instrument (Becton Dickinson Inc., Franklin Lakes, NJ, USA). Immunoreactivity of HYNIC-MT1-MMP mAb was evaluated with the median fluorescence intensity ratio to control mouse IgG$_3$ and compared with that of MT1-MMP mAb. Measurements were performed three times per rabbit using three JW rabbits.

Non-invasive imaging

After 12 h of fasting, rabbits were initially anaesthetized with ketamine (35 mg/kg, intramuscularly) and xylazine (5 mg/kg, intramuscularly). The anaesthetic state was maintained with additional doses of ketamine and xylazine during the experimental period. Rabbits were placed on the scanner bed in a prone position to include the abdominal aorta in the field of view. ^{99m}Tc-MT1-MMP mAb (140–741 MBq, 300 μg) was injected into the marginal ear vein of four WHHLMI rabbits and four control rabbits. At 10 min and 24 h after injection of the radiotracer, planar images were obtained for 10 min with a gamma camera (SPECT 2000H, Hitachi Medical Co., Tokyo, Japan) employing a low energy high resolution parallel-hole collimator with a spatial resolution of 6.7 mm in full-width at half-maximum (FWHM). Serial arterial blood samples were collected from an auricular artery. Similarly, imaging studies of ^{99m}Tc-IgG$_3$ were performed after the injection of ^{99m}Tc-IgG$_3$ (91–198 MBq, 300 μg) into the marginal ear vein of four WHHLMI rabbits. All rabbits were also applied to the biodistribution studies described below.

Biodistribution studies

Immediately after the non-invasive imaging studies, 24 h after tracer injection, the animals were sacrificed with an overdose of pentobarbital. The ascending-arch, thoracic and abdominal aortas, blood and other tissues were removed. The ascending-arch aortas were divided into six segments, while the thoracic and abdominal aortas were divided into nine segments (Fig. 1). Each segment was weighed and immediately fixed in a solution containing L-(+)-lysine hydrochloride (75 mM) and 4% paraformaldehyde in phosphate buffer (37.5 mM, pH 7.4). The radioactivity of each sample was measured with a well-type gamma counter (ARC-2000, Aloka, Tokyo, Japan). Results were expressed as the differential uptake ratio (DUR), which was calculated as (tissue activity/tissue weight)/(injected radiotracer activity/animal body weight), with activities given in becquerels and weights given in grams. The aorta to blood ratio (A/B ratio) and the aorta to muscle ratio (A/M ratio) were calculated from DUR values.

Autoradiography (ARG)

Autoradiographic studies were also performed using the aortas obtained at 24 h after tracer injection (the same aortas used in the biodistribution studies). A total of eight

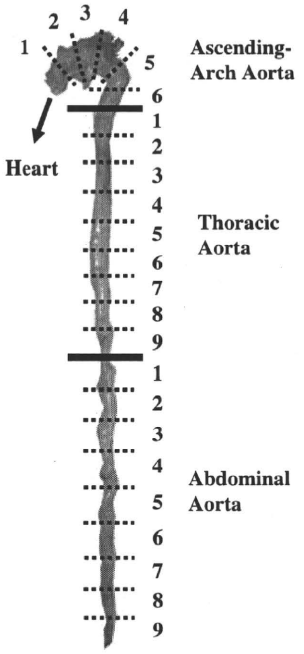

Fig. 1 Segmentation of the ascending-arch, thoracic and abdominal aortas. The ascending-arch aortas were divided into six segments, while the thoracic and abdominal aortas were divided into nine segments

segments, the second and fifth segments from the ascending-arch aorta, and the second, fifth and eighth segments from the thoracic and abdominal aortas, from each animal were used for autoradiographic studies. These segments were frozen and cut into 20-μm thick slices using a cryomicrotome. To obtain ^{99m}Tc-MT1-MMP mAb and ^{99m}Tc-IgG$_3$ autoradiograms, sections were thaw-mounted on silane-coated slides, which were then placed on a phosphor image plate (Fuji Imaging Plate BAS-UR, Fuji Photo Film, Tokyo, Japan) for 24 h together with calibrated standards ($^{99m}TcO_4^-$solution). The ARG images were analysed using a computerized imaging analysis system (Bio-Imaging Analyzer BAS2500 and Image Gauge Software, Fuji Photo Film, Tokyo, Japan). Radioactivity in each region of interest (ROI) was expressed as %ID×BW/mm^2, calculated as (radioactivity in ROI)/(injected radioactivity/animal body weight), with radioactivity in ROI given in becquerels/mm^2, injected activity given in becquerels and weight given in grams.

Histological analysis

Serial sections of ARG slices were subjected to histological analysis. Azan-Mallory staining, haematoxylin and eosin (H&E) staining and immunohistochemical staining (MT1-MMP, macrophage and smooth muscle cell) were performed. Immunohistochemical staining of MT1-MMP was carried out using the anti-MT1-MMP monoclonal IgG (MT1-MMP mAb, described above) and a Dako EnVision + kit (Dako, Tokyo, Japan) with haematoxylin counterstaining. In the same manner, immunohistochemical staining for macrophages and smooth muscle cells was carried out with a rabbit macrophage-specific mAb, RAM11 (Dako, Tokyo, Japan) and a human smooth muscle actin-specific mAb, 1A4 (Dako, Tokyo, Japan), respectively. Immunostaining with subclass-matched irrelevant IgG served as a negative control. Azan-Mallory staining and H&E staining were performed with standard procedures. Areas (μm^2) occupied by each lesion component were evaluated with a VHX Digital Microscope (Keyence Corp., Osaka, Japan). Collagen-rich fibres and extracellular lipid deposits (extracellular vacuoles and lacunae) were assessed with Azan-Mallory staining. Macrophage and smooth muscle cell areas were determined by immunohistochemical staining (RAM11 and 1A4). MT1-MMP expression density was assessed as a percentage of positively stained areas (% positive).

Classification of atherosclerotic lesions

The atherosclerotic lesions in WHHLMI rabbits were divided into four categories using a classification scheme based on the recommendations of the American Heart Association (AHA) [25, 26] by Azan-Mallory staining and H&E staining as previously described [27, 28] (Fig. 2a–p): (1) neointimal lesion (type I–III), (2) atheromatous lesion (type IV), (3) fibroatheromatous lesion (type Va, Vb) and (4) collagen-rich lesion (type Vc). Neointimal lesions were defined as having adaptive thickening of the intima consisting of mainly smooth muscle cells and few macrophages. Atheromatous lesions contained thin fibrous connective tissue and a dense accumulation of extracellular lipid and foam cells and were considered to be vulnerable-like lesions in human atherosclerotic plaques. Fibroatheromatous lesions were composed of several lipid cores, separated by thick layers of fibromuscular connective tissue, which was relatively stable to rupture [29]. Collagen-rich lesions consisted of a predominantly collagenous component and contained smooth muscle cells.

ROIs were placed to cover each atherosclerotic lesion in the aorta section of the WHHLMI rabbit and then transferred to the corresponding ARG images (Fig. 2q–v).

Statistical analysis

Data are presented as the mean ± SD. Statistical analysis was performed with the Kruskal-Wallis test with post hoc analysis by the Holm test (Table 1). Correlation coefficients were assessed by Spearman rank correlation coefficients (Fig. 4i, j). Comparisons among lesion types were performed using the Kruskal-Wallis test with post hoc analysis by the Holm test (Fig. 5a, b). A two-tailed value of $p<0.05$ was considered statistically significant.

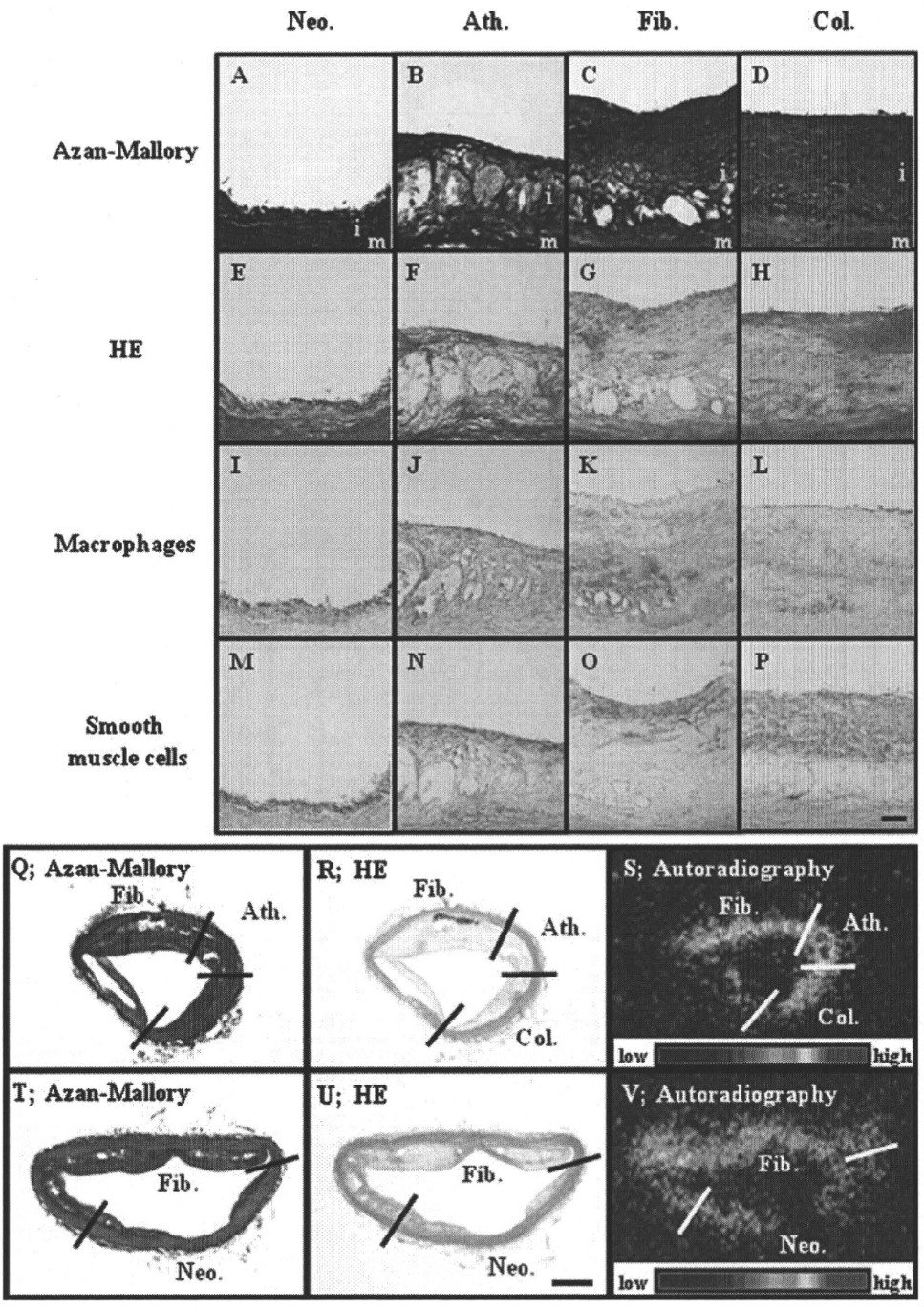

Fig. 2 Representative photomicrographs of histological features (**a**–**p**) and lesion classification (**q**–**v**) of atherosclerotic lesions in WHHLMI rabbits. Atherosclerotic lesions were microscopically divided into four categories as described in the "Materials and methods" section: neointimal lesion (*Neo.*, *left column*), atheromatous lesion (*Ath.*, *second column*), fibroatheromatous lesion (*Fib.*, *third column*) and collagen-rich lesion (*Col.*, *right column*). ROIs were placed to cover each atherosclerotic lesion in the aorta section of the WHHLMI rabbit and then transferred to the corresponding ARG images. *m* media, *i* intima, *bar* = 100 μm (**a**–**p**) and 1 mm (**q**–**v**)

Results

Immunoreactivity of HYNIC-MT1-MMP mAb

By FACS analysis, the signals of MT1-MMP mAb and HYNIC-MT1-MMP mAb were clearly distinct from that of the negative control IgG_3. The median fluorescence intensity ratios of MT1-MMP mAb and HYNIC-MT1-MMP mAb to control IgG_3 were 2.99±0.26 and 2.36±0.92, respectively, and the difference was not statistically significant (Kruskal-Wallis test).

Non-invasive imaging and biodistribution studies

Planar images showed primarily blood pool radioactivity in the abdominal aorta of every rabbit at 10 min after injection of ^{99m}Tc-MT1-MMP mAb or ^{99m}Tc-IgG_3 (Fig. 3a–c). At 24 h, the atherosclerotic abdominal aorta was clearly visible in the WHHLMI rabbits given ^{99m}Tc-MT1-MMP mAb with decreased blood pool radioactivity within the abdominal aorta (Fig. 3d–f). Relatively high ^{99m}Tc-MT1-MMP mAb accumulations were found in the liver, spleen and kidneys of both WHHLMI and control rabbits.